Fasting-mimicking diet and hormone therapy modulate metabolic factors to promote breast cancer regression

By Irene Caffa[1,2]*, Vanessa Spagnolo[3,4]*, Claudio Vernieri[4,5], Francesca Valdemarin[1,2], Min Wei[6], Sebastian Brandhorst[6], Chiara Zucal[7], Pamela Becherini[1,2], Else Driehuis[8], Lorenzo Ferrando[1], Luca Mastracci[2,9], Alberto Tagliafico[10], Michele Cilli[2], Valerio G. Vellone[2,9], Silvano Piazza[7], Francesco Piacente[1,2], Anna Laura Cremonini[1,2], Raffaella Gradaschi[2], Carolina Mantero[2], Gabriele Zoppoli[1,2], Michele Cea[1,2], Mario Passalacqua[11], Annalisa Arrighi[12], Patrizio Odetti[1,2], Fiammetta Monacelli[1,2], Giulia Salvadori[3,4], Salvatore Cortellino[4], Hans Clevers[8], Samir G. Sukkar[2], Filippo De Braud[3,5], Alessandro Provenzani[7], Valter D. Longo[4,6]#, and Alessio Nencioni[1,2]#.

From the [1]Department of Internal Medicine and Medical Specialties, University of Genoa, Viale Benedetto XV 6, 16132 Genoa, Italy;
the [2]IRCCS Ospedale Policlinico San Martino, Largo Rosanna Benzi 10, 16132 Genoa, Italy;
the [3]Department of Oncology and Hemato-oncology, University of Milan, Milan, Italy;
the [4]IFOM, FIRC Institute of Molecular Oncology, Milan, Italy;
the [5]Fondazione IRCCS Istituto Nazionale dei Tumori, Milan, Italy;
the [6]Longevity Institute and Davis School of Gerontology, University of Southern California, Los Angeles, CA, US.
the [7]Hubrecht Institute, Royal Netherlands Academy of Arts and Sciences, 3584 CT Utrecht, The Netherlands
the [8]Center For Integrative Biology (CIBIO), University of Trento, via Sommarive 9, Trento, Italy;
the [9]Department of Integrated, Surgical and Diagnostic Sciences (DISC), University of Genoa, Largo Rosanna Benzi 8, 16132 Genoa, Italy;
the [10]Department of Health Sciences (DISSAL), University of Genoa, 16132 Genoa, Italy;
the [11]Department of Experimental Medicine and CEBR, University of Genoa, Viale Benedetto XV 1, 16132 Genoa, Italy;
and the [12]Department of Neuroscience, Rehabilitation, Ophthalmology, Genetics and Maternal-Infantile Sciences, University of Genoa, Italy.

*These authors contributed equally to this work
#These authors contributed equally to this work

To whom correspondence should be addressed:
Dr. Alessio Nencioni, Department of Internal Medicine, University of Genoa, Viale Benedetto XV 6, 16132 Genoa, Italy; Phone: +39 010 353 8990; Fax +39 010 353 7989; Email: alessio.nencioni@unige.it.
Dr. Valter D. Longo, IFOM, FIRC Institute of Molecular Oncology, Via Adamello 16, 20139, Milano, Italy and Longevity Institute, School of Gerontology, Department of Biological Sciences, University of Southern California, 3715 McClintock Avenue, Los Angeles, CA 90089-0191, USA; Email: vlongo@usc.edu.

Abstract

Breast cancer (BC) is the most common malignancy in women with 1.7 million new diagnoses/year and is responsible for more than 450,000 yearly deaths worldwide[1,2]. The approximately 75% of BC which express the estrogen receptor (ER) and/or progesterone receptor are referred to as hormone receptor-positive (HR+) BC. Endocrine therapy (ET) is usually active in these tumors, although drug resistance limits its benefit[1,3]. Here we show that in HR+ BC models, periodic cycles of fasting or fasting-mimicking diet (FMD) enhance tamoxifen (TMX) and fulvestrant (FULV) activity by lowering circulating IGF-1, insulin, and leptin levels, and by blocking AKT-mTOR signaling via EGR1 and PTEN upregulation. When FULV is combined with palbociclib (a cyclin-dependent kinase 4/6 inhibitor), addition of periodic FMD cycles promotes long-lasting tumor regressions and reverts acquired resistance to this regime. Both fasting and FMD prevent TMX-induced endometrial hyperplasia. In BC patients receiving ET, FMD cycles cause changes analogous to those observed in mice, including reduced leptin and IGF-1 levels, which remain low for extended periods. In mice, these long-lasting effects were associated with carryover anticancer activity. These results support the conduction of large prospective studies of periodic FMD as an adjuvant to ET in patients with HR+ BC.

Growth factor signaling, i.e. PI3K/AKT/mammalian target of rapamycin (mTOR) and MAP kinase signaling, enhances ER activity and is also a key mechanism underlying endocrine resistance[1,3,4]. Water-only fasting (fasting) or plant-based, low-calorie, carbohydrate- and protein-restricted FMDs reduce circulating GFs, such as insulin and IGF-1[3-5]. Therefore, we hypothesized that these dietary interventions could be used to enhance the activity of ET and delay endocrine resistance.

Low-serum and low-glucose culture conditions designed to mimic the effects of fasting/FMD (short-term starvation - STS - conditions) increased the antitumor activity of TMX or FULV in HR+/HER2- BC cell lines, and similar results were obtained in mouse xenografts of the same cell lines with weekly cycles of fasting or FMD (Fig.1a-c, Extended Data Fig.1a-g). The enhancement of ET activity through STS-conditions was dependent on the reduction in serum rather than glucose since adding back the latter did not affect the observed potentiation (Extended Data Fig.1h). Moreover, STS-conditions increased the antitumor activity of TMX in tumor organoids from patients with HR+ BC[6] and weekly cycles of FMD prevented acquired resistance to TMX in mice (Fig.1d-e).

In addition to increasing β-hydroxybutyrate levels (Fig.1f) and to lowering blood glucose (from 6.3±0.6 mmol/l to 4.1±0.3 mmol/l and 4.0±0.9 mmol/l with fasting and FMD, respectively; n=4) fasting and FMD w/ or w/o ET significantly modified circulating growth factors levels (Fig.1g). Serum c-peptide (a proxy of endogenous insulin production) was blunted by both dietary interventions. Fasting and FMD reduced both circulating Igf1 and Igfbp3 (which binds more than 80% of circulating Igf1 and protects it from rapid degradation[7]), while increasing Igfbp1 (which inhibits Igf1 action by binding to Igf1 itself and preventing its binding to Igf receptors[7]). Thus, the combined effect of these diets was a marked reduction in Igf1 levels and bioavailability. The levels of leptin, an adipokine that acts as a growth factor for BC cells and reduces ET efficacy[8-10], were only reduced when fasting or FMD were combined with ET. Adiponectin, which exerts antitumor effects[9], was only affected by the combination of fasting and TMX (Extended Data Fig.1i). To define the role of insulin, leptin, and IGF-1 in the FMD-induced potentiation of ET antitumor effects, we administered each of these factors, which we refer to as Fasting-Reduced Factors (FRFs) to MCF7 xenograft-bearing mice, that were being treated with FULV plus FMD (Fig.1h, Extended Data Fig.1l). Adding back any of these factors (or their combination) was sufficient to revert the enhancement of FULV activity through the FMD (Fig. 1h). Withdrawing the FRFs restored tumor

sensitivity to ET and FMD, while administering them to mice that had only received FULV plus FMD stimulated tumor growth and abrogated the FMD-induced potentiation of FULV (Fig. 1h, after crossover). These data confirm the key role of insulin reduction in the enhancement of ET antitumor activity through fasting/FMD[11]. However, they show that the simultaneous reduction of additional factors with growth-promoting ability through these dietary interventions is necessary for this therapeutic effect to be achieved. The fact that all these FRFs have overlapping effects in the activation of signaling cascades regulating HR+ BC sensitivity to ET, and in particular the PI3K-AKT-mTOR pathway[8,9,11-14], may explain why reducing all three is required for the promoting of ET antitumor activity. Consistent with this notion, tumors isolated from mice, from which FRFs were withdrawn, exhibited reduced phosphorylation of AKT and of p70S6K (a mTOR target), while in tumors from animals administered FRFs during treatment with FULV plus FMD, we found levels of AKT and p70S6K phosphorylation that were comparable to those of *ad lib*. fed mice (Fig.1i).

We monitored the effect of fasting/FMD on additional circulating factors with a reported role in BC pathophysiology[14], and found that both fasting and FMD (w/ or w/o TMX/FULV) downregulated Tnf, which acts pro-oncogenically by upregulating aromatase in the tumor microenvironment and by enhancing angiogenesis and cell invasion, and Il1β, which enhances HR^+ BC cell migration and metastasis[14,15] (Extended Data Fig.1i). Since insulin, Igf1, and leptin down-regulation proved essential for the potentiation of ET activity via FMD, we focused on these FRFs for subsequent mechanistic experiments, although it is likely that the benefit of fasting/FMD to ET may involve other mediators, such as Tnf and Il1β.

STS-conditions and the FMD (in experiments with MCF7 xenografts) cooperated with ET to increase the expression of PTEN, which is an upstream negative regulator of AKT-mTOR signaling, in HR+ BC cell lines and in HR+/HER2- BC organoids (Fig.2a-c, Extended Data Fig. 2a). In line with the previously described reduction of AKT phosphorylation and mTOR activity (Fig.1i), these treatment combinations reduced levels of phosphorylated p70S6K and eIF4E, increased the translational repressor 4E-BP1, primarily in its unphosphorylated form, and inhibited protein synthesis (Fig.2a,b and Extended Data Fig. 2a-d). Among the known enhancers of PTEN expression, we focused on the tumor suppressor EGR1 (whose expression is associated with good prognosis in BC patients[16,17]) since we previously showed that EGR1 becomes upregulated in healthy tissues during fasting[18] and because EGR1 was also reported to be suppressed by ER activity[19]. EGR1 was elevated upon combined treatment of HR+ BC cell lines and of BC organoids (Fig.2a-c and Extended Data Fig.2a,b). Its silencing reduced the antitumor activity of coupled STS-conditions and ET and prevented PTEN accumulation and the reduction in AKT phosphorylation in response to this combination (Fig.2d,e and Extended Data Fig.2e-g). BC cell protection from combined ET and STS through EGR1 silencing reflected persistent AKT activity, since the AKT inhibitors, GDC0068 and AZD5363, and the PI3K inhibitor, LY294002, all abolished such protection (Fig.2f). PTEN silencing and myr-AKT overexpression also reduced MCF7 sensitivity to combined ET and STS/FMD (Fig.2g,h; and Extended Data Fig.2h). Supplementation with insulin, IGF-1 and leptin, or with 17β-estradiol prevented the increase in EGR1, PTEN and 4E-PBP1, that were induced by combined TMX and STS-conditions in MCF7 cells (Fig.2i). In addition, EGR1 upregulation was also abolished by constitutively active, myristoylated AKT (Fig.2l). Therefore, fasting/FMD and ET cooperate, at least in part, via a mechanism, whereby EGR1 becomes upregulated in BC cells due to AKT inhibition, causes PTEN upregulation and is crucial for maintaining AKT inhibition itself. AMP-activated kinase (AMPK), which negatively controls mTOR activity, was also phosphorylated on an activating residue in BC cells that were exposed to combined ET and STS-conditions (Extended Data Fig.2a,b). This effect was prevented by both PTEN silencing and myr-AKT expression (Extended Data Fig.3), indicating that AMPK stimulation

in response to coupled ET and STS-conditions is secondary to PTEN upregulation and to reduced AKT activity[20].

ER activity is essential for HR+ BC cell survival and proliferation, and is enhanced by insulin, IGF-1 and leptin signaling at multiple levels[1,5,8,13,21]. STS-conditions reduced ER transcriptional activity and enhanced FULV- and TMX-mediated ER inhibition in HR+ BC cell lines as detected by luciferase reporter assays and by monitoring the expression of the ER target genes *TFF1*, *PGR*, and *GREB1* (Fig.2m,n). *TFF1* was also downregulated via combined TMX and STS in HR+ BC organoids (Fig.2o). Thus, STS-conditions and ET also cooperate in terms of ER activity inhibition. Using gene expression microarrays and Gene Set Enrichment Analysis (GSEA), we found a downregulation of gene categories belonging to cell cycle-related themes through combined TMX and STS-conditions in MCF7 (Fig.3a and Extended Data Fig.4a,b). We verified E2F1, E2F2, CCNE1 and CCND1 downregulation after combined treatment at the mRNA (Fig.3b and Extended Data Fig.4c) and at the protein level (CCND1; Figure 3c,d). Consistent with their effects on cell cycle regulators, STS and ET together reduced phosphorylated RB in HR+ BC cells and induced cell cycle arrest in the G0-G1 phase (Fig.3c and Extended Data Fig.4d-f). EGR1 silencing and myr-AKT expression both attenuated CCND1 downregulation in response to coupled ET and STS-conditions, and myr-AKT also protected MCF7 from the cell cycle arrest imposed by ET, STS and their combination (Fig.3e,f). Therefore, EGR1 and AKT act upstream to mediate CCND1 downregulation through combined ET and STS and the consequent cell cycle arrest.

Thereafter, we reasoned that CCND1 downregulation via the combination of ET and STS could be exploited to provide an additional therapeutic effect, by adding the CDK4/6 inhibitor, palbociclib (PALB; Fig.3g). In orthotopic MCF7 xenografts-bearing mice (n=15-18 mice/arm), FMD or PALB postponed the occurrence of resistance to FULV in a similar way (Fig.3h). However, even with these combinations, resistance acquisition and tumor progression could not be avoided. In contrast, combining FULV, FMD and PALB not only prevented tumor growth for over 160 days, but it also led to a slow, but steady, tumor shrinkage. Furthermore, administering FMD cycles to mice with tumours that had already become resistant to FULV plus PALB induced tumor shrinkage even at this advanced stage (Fig. 3i). The ability of MCF7 from resistant tumors to grow in the presence of FULV and PALB was verified *in vitro* and *in vivo* (Fig.3i and Extended Data Fig.4g,h). Resistant MCF7 were used to establish new xenografts, and, again, adding the FMD to FULV and PALB resulted in antitumor activity against these re-transplants (Fig.3i, right panel).

Necropsies of mice treated with TMX in combination with fasting/FMD demonstrated *uteri* of smaller size as compared to the enlarged *uteri* observed in mice receiving TMX alone. In dedicated experiments, we found that both fasting and FMD prevented the increase in *uterus* size and weight caused by a four-week TMX treatment (Extended Data Fig.5a; n= 5-8 mice/arm), and reduced the histological signs of TMX-induced endometrial hyperplasia (Extended Data Fig.5b,c). Fasting/FMD w/ or w/o TMX reduced *Tff1* expression (a proxy for ER activity) and phosphorylated AKT in mouse *uteri*, while increasing *Egr1* and *Pten* mRNA (Extended Data Fig.5d,e). Pten and Egr1 protein were also upregulated in the *uterus* in response to water only fasting, whereas only a trend towards an increase in these proteins through FMD was observed. Therefore, both fasting and FMD reduce TMX-induced endometrial hyperplasia, ER activity and AKT activation in the mouse *uterus*. Pten and Egr1 upregulation are likely to be involved in AKT inhibition in the *uterus* via fasting, whereas FMD-mediated AKT inhibition in this organ may reflect other mechanisms. Finally, fasting/FMD cooperated with TMX to reduce mouse intra-abdominal fat (Extended Data Fig.5f). Since intra-abdominal adipose tissue is a major source of adipokines, this effect could also explain the leptin-lowering effect, that is obtained by combining ET with periodic fasting/FMD (Fig.1g).

We tested the combination of FMD and ET in 36 patients with HR+ BC, who were enrolled in the NCT03595540 (pt.#1-24) or in the NCT03340935 (pt.#25-36) clinical trials. In the former trial,

which utilizes a previously reported 5-day FMD[22,23], patients received on average 6.1 FMD cycles, with some of them receiving up to 13 cycles. Also in this trial, the FMD proved to be safe, only leading to G1-2 adverse events, most commonly headache (41%) and fatigue (21%) (Extended Data Table 1 and 2). Patients from the NCT03340935 study received a similar, albeit more calorie-restricted FMD, and completed an average of 5.5 cycles in the absence of severe adverse events (Extended Data Table 1). Patients from the NCT03595540 trial (who received dietary recommendations as per international guidelines[24,25] and instructions for physical activity for the intervals between FMD cycles) maintained stable body weight and hand grip (Fig.4a,b). Their bioimpedance phase angle[26] and fat-free mass increased significantly over time, while their fat mass decreased (Fig.4c-e). These findings were confirmed by abdominal or thoracic CT scan analyses in those patients for whom CT scans were available at baseline and during treatment (Fig.4f). Clinical outcomes in patients with metastatic HR+/HER2- BC, including those treated with combined ET, PALB and FMD (n=4), are remarkable (Fig.4g and Extended Data Table 2). Pt.#1, #26 and #27 have been treated in the second-line treatment setting for 30, 18 and 11 months, respectively, receiving a total of 10 (Pt.#1) and 8 (Pt.#26, #27) FMD cycles (median progression-free survival in this clinical context is 9 months[15,27]). P.#1 and Pt.#26 still have SD, while Pt.#27 progressed after 11 months[15,27]. Pt.#29 received fourth-line treatment with FULV and PALB plus 5 FMD cycles, ultimately progressing after 11 months. Considering all patients with HR+/HER2- BC enrolled in these trials, the FMD increased circulating ketone bodies, lowered blood glucose, serum IGF-1, leptin, and c-peptide (Fig.4h and Extended Data Fig.6a). Leptin and IGF-1 (but not c-peptide) levels were still lower than the baseline values three weeks after the end of the FMD (Fig.4i).

Similar findings were obtained in mice (Fig.4l and Extended data Fig.7b), where, in response to combined FMD and ET (but not to FMD or ET alone), leptin and IGF-1 (but not c-peptide) remained lower despite refeeding one week after the end of the FMD as compared to *ad lib*. fed mice. Since both leptin and IGF-1 stimulate BC cell proliferation[8,13,21,28,29], we evaluated whether these changes in circulating FRFs, persisting beyond the FMD period, were associated with anticancer effects. A one-month treatment of MCF7 xenograft-bearing mice with coupled ET and FMD (or fasting), but not with the single treatments, slowed tumor growth for up to 90 days after treatment withdrawal, enhancing mouse survival (Fig.4m and Extended data Fig.7c,d). In addition, mouse pre-treatment with coupled ET and FMD for one month, followed by MCF7 cell inoculation, reduced tumor engraftment and slowed the growth of those tumors that did engraft (Fig.4n,o). Pre-treatment with FULV also slowed MCF7 xenograft growth, likely due to the use of a long-acting formulation of this agent in our study. However, pre-treatment with combined FMD and FULV was more active than FULV alone.

In conclusion, periodic cycles of fasting/FMD increase the anti-cancer activity of TMX and FULV, delay resistance to these agents and, in combination with FULV and PALB, cause tumor regression and reverse acquired resistance to these two drugs. Pivotal for the cooperation between fasting/FMD and ET appears to be the simultaneous reduction in blood IGF-1, insulin and leptin levels, with the consequent inhibition of the PI3K-AKT-mTOR signalling pathway, at least in part via EGR1 and PTEN upregulation (Fig.3g). Of note, fasting/FMD provide AKT-mTOR axis inhibition without causing rebound hyperglycemia and hyperinsulinemia that are instead associated with the use of pharmacologic inhibitors of PI3K or mTORC1, and which have been implicated in tumor resistance to these treatment[11,30,31]. The leptin- and IGF-1-lowering effect of FMD plus ET persists beyond the FMD period, and is associated with carryover anticancer activity. Therefore, the observed regression of HR+ BCs in mice could result from the combination of an acute, more significant reduction of FRFs, and a milder, chronic reduction in FRFs. In fact, the long term reduction in leptin and IGF-1 may contribute to generate an extended inhospitable environment for

HR+ BC cells. The prevention of TMX-induced endometrial hyperplasia through fasting/FMD is promising given the prevalence of this side effect of TMX and the limited options for preventing it[1,32]. Thus, these findings define a possible, additional adverse event-related application for these dietary regimens in women treated with TMX.

Overall, our results provide the rationale for conducting clinical studies of fasting-based dietary strategies as a means to delay resistance to ET w/ or w/o CDK4/6 inhibitors in HR+ BC and to prevent TMX-induced endometrial hyperplasia.

References

1 DeVita, V. J., Laurence, TS. , Rosenberg, SA. . DeVita, Hellmann and Rosenberg's cancer: principles & practice of oncology. 11th edn, 1269-1316 (Wolters Kluwer, 2019).

2 Ferlay, J. et al. Cancer incidence and mortality worldwide: sources, methods and major patterns in GLOBOCAN 2012. International journal of cancer 136, E359-386, doi:10.1002/ijc.29210 (2015).

3 Araki, K. & Miyoshi, Y. Mechanism of resistance to endocrine therapy in breast cancer: the important role of PI3K/Akt/mTOR in estrogen receptor-positive, HER2-negative breast cancer. Breast cancer 25, 392-401, doi:10.1007/s12282-017-0812-x (2018).

4 AlFakeeh, A. & Brezden-Masley, C. Overcoming endocrine resistance in hormone receptor-positive breast cancer. Current oncology 25, S18-S27, doi:10.3747/co.25.3752 (2018).

5 Lee, A. V., Cui, X. & Oesterreich, S. Cross-talk among estrogen receptor, epidermal growth factor, and insulin-like growth factor signaling in breast cancer. Clinical cancer research : an official journal of the American Association for Cancer Research 7, 4429s-4435s; discussion 4411s-4412s (2001).

6 Sachs, N. et al. A Living Biobank of Breast Cancer Organoids Captures Disease Heterogeneity. Cell 172, 373-386 e310, doi:10.1016/j.cell.2017.11.010 (2018).

7 Jones, J. I. & Clemmons, D. R. Insulin-like growth factors and their binding proteins: biological actions. Endocrine reviews 16, 3-34, doi:10.1210/edrv-16-1-3 (1995).

8 Sanchez-Jimenez, F., Perez-Perez, A., de la Cruz-Merino, L. & Sanchez-Margalet, V. Obesity and Breast Cancer: Role of Leptin. Frontiers in oncology 9, 596, doi:10.3389/fonc.2019.00596 (2019).

9 Garofalo, C., Sisci, D. & Surmacz, E. Leptin interferes with the effects of the antiestrogen ICI 182,780 in MCF-7 breast cancer cells. Clinical cancer research : an official journal of the American Association for Cancer Research 10, 6466-6475, doi:10.1158/1078-0432.CCR-04-0203 (2004).

10 Bougaret, L. et al. Adipocyte/breast cancer cell crosstalk in obesity interferes with the anti-proliferative efficacy of tamoxifen. PloS one 13, e0191571, doi:10.1371/journal.pone.0191571 (2018).

11 Pollak, M. The insulin and insulin-like growth factor receptor family in neoplasia: an update. Nature reviews. Cancer 12, 159-169, doi:10.1038/nrc3215 (2012).

12 Jarde, T., Perrier, S., Vasson, M. P. & Caldefie-Chezet, F. Molecular mechanisms of leptin and adiponectin in breast cancer. European journal of cancer 47, 33-43, doi:10.1016/j.ejca.2010.09.005 (2011).

13 Saxena, N. K. et al. Concomitant activation of the JAK/STAT, PI3K/AKT, and ERK signaling is involved in leptin-mediated promotion of invasion and migration of hepatocellular carcinoma cells. Cancer research 67, 2497-2507, doi:10.1158/0008-5472.CAN-06-3075 (2007).

14 Hopkins, B. D. et al. Suppression of insulin feedback enhances the efficacy of PI3K inhibitors. Nature 560, 499-503, doi:10.1038/s41586-018-0343-4 (2018).

15 Cristofanilli, M. et al. Fulvestrant plus palbociclib versus fulvestrant plus placebo for treatment of hormone-receptor-positive, HER2-negative metastatic breast cancer that progressed on previous endocrine therapy (PALOMA-3): final analysis of the multicentre, double-blind, phase 3 randomised controlled trial. The Lancet. Oncology 17, 425-439, doi:10.1016/S1470-2045(15)00613-0 (2016).

16 Lasham, A. et al. A novel EGR-1 dependent mechanism for YB-1 modulation of paclitaxel response in a triple negative breast cancer cell line. International journal of cancer 139, 1157-1170, doi:10.1002/ijc.30137 (2016).

17 Shajahan-Haq, A. N. et al. EGR1 regulates cellular metabolism and survival in endocrine resistant breast cancer. Oncotarget 8, 96865-96884, doi:10.18632/oncotarget.18292 (2017).

18 Di Biase, S. et al. Fasting regulates EGR1 and protects from glucose- and dexamethasone-dependent sensitization to chemotherapy. PLoS Biol 15, e2001951, doi:10.1371/journal.pbio.2001951 (2017).

19 Di Leva, G. et al. Estrogen mediated-activation of miR-191/425 cluster modulates tumorigenicity of breast cancer cells depending on estrogen receptor status. PLoS Genet 9, e1003311, doi:10.1371/journal.pgen.1003311 (2013).

20 Hawley, S. A. et al. Phosphorylation by Akt within the ST loop of AMPK-alpha1 down-regulates its activation in tumour cells. The Biochemical journal 459, 275-287, doi:10.1042/BJ20131344 (2014).
21 Ando, S., Barone, I., Giordano, C., Bonofiglio, D. & Catalano, S. The Multifaceted Mechanism of Leptin Signaling within Tumor Microenvironment in Driving Breast Cancer Growth and Progression. Frontiers in oncology 4, 340, doi:10.3389/fonc.2014.00340 (2014).
22 Brandhorst, S. et al. A Periodic Diet that Mimics Fasting Promotes Multi-System Regeneration, Enhanced Cognitive Performance, and Healthspan. Cell metabolism 22, 86-99, doi:10.1016/j.cmet.2015.05.012 (2015).
23 Wei, M. et al. Fasting-mimicking diet and markers/risk factors for aging, diabetes, cancer, and cardiovascular disease. Sci Transl Med 9, doi:10.1126/scitranslmed.aai8700 (2017).
24 Arends, J. et al. ESPEN guidelines on nutrition in cancer patients. Clin Nutr 36, 11-48, doi:10.1016/j.clnu.2016.07.015 (2017).
25 Arends, J. et al. ESPEN expert group recommendations for action against cancer-related malnutrition. Clin Nutr 36, 1187-1196, doi:10.1016/j.clnu.2017.06.017 (2017).
26 Grundmann, O., Yoon, S. L. & Williams, J. J. The value of bioelectrical impedance analysis and phase angle in the evaluation of malnutrition and quality of life in cancer patients--a comprehensive review. European journal of clinical nutrition 69, 1290-1297, doi:10.1038/ejcn.2015.126 (2015).
27 Turner, N. C. et al. Palbociclib in Hormone-Receptor-Positive Advanced Breast Cancer. The New England journal of medicine 373, 209-219, doi:10.1056/NEJMoa1505270 (2015).
28 Creighton, C. J. et al. Insulin-like growth factor-I activates gene transcription programs strongly associated with poor breast cancer prognosis. Journal of clinical oncology : official journal of the American Society of Clinical Oncology 26, 4078-4085, doi:10.1200/JCO.2007.13.4429 (2008).
29 Karey, K. P. & Sirbasku, D. A. Differential responsiveness of human breast cancer cell lines MCF-7 and T47D to growth factors and 17 beta-estradiol. Cancer research 48, 4083-4092 (1988).
30 Baselga, J. et al. Everolimus in postmenopausal hormone-receptor-positive advanced breast cancer. The New England journal of medicine 366, 520-529, doi:10.1056/NEJMoa1109653 (2012).
31 Andre, F. et al. Alpelisib for PIK3CA-Mutated, Hormone Receptor-Positive Advanced Breast Cancer. The New England journal of medicine 380, 1929-1940, doi:10.1056/NEJMoa1813904 (2019).
32 Hu, R., Hilakivi-Clarke, L. & Clarke, R. Molecular mechanisms of tamoxifen-associated endometrial cancer (Review). Oncology letters 9, 1495-1501, doi:10.3892/ol.2015.2962 (2015).

Figure Legends

Figure 1. Fasting/FMD potentiate the activity of ET in HR+ BC via reduction of circulating growth factors. a-c Growth of MCF7, ZR-75-1 and T47D xenografts in mice were treated with TMX, FULV, weekly 48h fasting or FMD or combined ET and fasting/FMD. d, Primary HR+ BC organoids were treated with TMX w/ or w/o STS conditions for 72h before being imaged and before quantification of their viability. e, MCF7 xenograft growth and corresponding mouse survival in response to prolonged TMX administration, weekly FMD, or their combination. f, g, β-serum hydroxibutyrate, Igf1, Igfbp1, Igfbp3, leptin and c-peptide concentration (fold change vs. baseline for circulating proteins) in six- to eight-week-old BALB/c athymic mice (nu+/nu+) before and after a 48h fasting/FMD (or ad lib. diet) and concomitant treatment w/ or w/o TMX/FULV. h, i, MCF7 xenograft growth in six- to eight-week-old BALB/c athymic mice (nu+/nu+) treated w/ or w/o FULV, FULV plus weekly FMD, or combination of FULV, weekly FMD and i.p. insulin, IGF-1, leptin, or the three GFs combined. At day 35 (crossover), GF administration was withdrawn, while it was started in mice that had only received FULV plus FMD. At the end of the experiments, phosphorylated AKT, p70S6K and vinculin in tumor masses were detected by Western blotting.

Figure. 2. Fasting/FMD and ETs cooperate to inhibit PI3K/AKT/mTOR signaling ER and in HR+ BC cells. a, b, PI3K/AKT/mTOR signaling and EGR1 and PTEN levels in MCF7 treated with FULV, FMD (in MCF7 xenografts), STS-conditions (in vitro experiments), or their combinations. c, EGR1 and PTEN expression in primary HR+ BC organoids treated with TMX, STS-conditions or their combination. d, e, Cell viability, PTEN levels, and AKT phosphorylation in MCF7 cells in response to EGR1 silencing, TMX, FULV, STS conditions, or their combination. f, Viability of control and of EGR1-silenced MCF7 in response to TMX, STS conditions, GDC0068, AZD5363, LY294002, or their combinations. g, MCF7 cell viability in response to myr-AKT overexpression, TMX, FULV, STS conditions, or their combination. h, in vivo growth of MCF7 with silenced EGR1 or PTEN, or with myr-AKT overexpression in response to FULV plus FMD. i, EGR1, PTEN and 4E-BP1 levels in MCF7 treated w/ or w/o STS conditions and TMX, the combination of insulin, IGF-1 and leptin, or 17β-estradiol. l, EGR1 and GADPH levels in MCF7 w/ or w/o myr-AKT overexpression. m-o, ER transcriptional activity and ER target gene expression in MCF7 and in HR+ BC organoids in response to TMX, FULV, STS conditions and their combinations.

Figure. 3. Cyclin D1 regulation and prevention of resistance to combined fulvestrant and palbociclib in HR+ BC through FMD. a-d, G1/S transition-promoting gene down-regulation with combined ET and STS in MCF7 cells as shown by GSEA, QPCR and WB *in vitro* and *in vivo*. c, Effect of TMX, FULV, STS conditions on CCND1 and RB phosphorylation as detected by Western blotting in MCF7 cells. d, Effect of FULV, FMD or their combination in MCF7 xenografts. E, Effect of EGR1 silencing, myr-AKT overexpression, FULV, STS conditions or their combinations on CCND1 expression in MCF7 cells. f, Cell-cycle analysis of control and myr-AKT-overexpressing MCF7 treated with ET, STS or their combinations. g, Putative model for the cooperation between fasting/FMD and ET at the level of PI3K-AKT-mTOR signaling and of CCND1 regulation. h, MCF7-xenograft growth and PFS in six-to-eight week old NOD/SCID mice treated with FULV, FMD, palbociclib or their combinations. i, In vivo response to weekly FMD of MCF7 xenografts with acquired resistance to FLUV+palbociclib (PALB) (left panel); response of re-transplanted, resistant MCF7 cells and of parental MCF7 to combined FULV and PALB w/ or w/o weekly FMD.

Figure 4. Effects of periodic FMD on body composition, circulating growth factors and disease in patients with HR+ BC and in mice. a-f, Body weight, hand grip, phase angle, fat-free and fat mass (n=23); , and muscle area (highlighted in red) quantification at L3 level (pt.#1) and at the Louis sternal angle (pt.#3) level in BC patients treated with ET and periodic FMD (NCT03595540 study). g, Representative PET scans from a patient from the NCT03340935 trial treated with the combination FMD, FULV and PALB. h, i, serum IGF-1, IGFBP1, IFGBP3, leptin, c-peptide, and ketone bodies before and immediately after a FMD cycle (h; n=6) and before and at the end of a FMD cycle (I; n=23) in BC patients treated with ET and FMD (NCT03595540 trial). l, Leptin levels in serum from mice treated with FULV, TMX, weekly FMD or their combination for two weeks, one week after the end of the last FMD cycle (n=6 mice/group). m, MCF7 xenograft growth

after a one-month treatment w/ or w/o TMX, FULV, FMD or their combination followed by observation. n, o, MCF7 engraftment and growth in six- to eight-week-old BALB/c athymic mice (nu+/nu+; n=6 mice/group) that were pre-treated for one month with TMX, FULV, FMD or their combinations, followed by MCF7 cell inoculation one week after the end of pre-treatment.

Methods

Cell Lines and Reagents

MCF7 and T47D cell lines were purchased from ATCC (LGC Standards S.r.l., Milan, Italy), ZR-75-1 cell line was a kind gift of Dr. Barbieri from the CBA of Genoa, Italy. Cells were passaged for less than 6 months before resuscitation for this study. These cell lines were authenticated at ATCC by analysis of eight short tandem repeat loci (CSF1PO, D13S317, D16S539, D5S818, D7S820, TH01, TPOX, and vWA) and of the Amelogenin gene (see the provider's web page). MCF7 and T47D cell lines were maintained in DMEM medium supplemented with 10% FBS, penicillin (50 units/ml), and streptomycin (50 µg/ml) (LifeTechnologies, Italy). ZR-75-1 cell line was maintained in DMEM medium supplemented with 10% FBS, penicillin (50 units/ml), and streptomycin (50 µg/ml) (LifeTechnologies, Italy). Recombinant human IGF-1 and recombinant human leptin were purchased from Peprotech (London, UK). Insulin (Humulin R) was obtained from the pharmacy of the IRCCS Ospedale Policlinico San Martino (Genoa, Italy). Puromycin, protease/phosphatase inhibitor cocktail, β-estradiol, sulforhodamine B, TMX and FULV (for in vitro use) were purchased from Sigma Aldrich S.r.l. (Milan, Italy). Fulvestrant for in vivo use was purchased from Astrazeneca (Italy; Faslodex). PALB for *in vitro* experiments was purchased from Selleck Chemicals while for *in vivo* experiments it was purchased from Medchem Express. 17β-estradiol-releasing pellets were purchased from Innovative Research of America (Sarasota, FL, USA).

Cell viability assays and cell doubling time estimation

$2.8x10^3$ MCF7, $5x10^3$ T47D or $5x10^3$ ZR-75-1 cells were plated in 96 well plates in CTR medium. After 24h medium was removed, cells were washed with PBS and incubated either in CTR (10% FCS and 1g/L glucose) or STS (1% FBS, 0,5g/L glucose) medium. After 24h cells were stimulated w/ or w/o with TMX or FULV at the indicated concentrations. Viability was determined 72h later by CellTiter96 Aqueous1 (Promega) according to the manufacturer's instructions. Where indicated IGF-1, recombinant human leptin and insulin were added to the culture medium at 5 ng/ml, 50 ng/ml and 10 µg/ml, respectively. Cell doubling time was estimated in vitro as described elsewhere50.

Organoid culture and viability assays

The organoid lines used were previously published by Sachs et al. and were cultured and passaged as previously described[6]. In viability assays, organoids were transferred to medium containing all the growth factors as previously described, except having RPMI 1640 without glucose as a base (instead of Advanced DMEM/F12). Glucose concentration was brought to 3 g/L for unstarved condition and to 0.5 g/L for STS condition while the concentration of B27 in STS medium was brought to 0.1x instead of $1x^6$. Four days after passaging, organoids were collected from the basement membrane extract (BME) by a 30 minutes incubation with 2u/mL dispase II (Sigma-Aldrich, cat. no. D4693) at 37^0C. Organoids/BME filtered with a 70 µm nylon filter (Falcon). Subsequently, organoids were brought to a $7.5x10^3$ organoids/mL density in medium containing 5% BME. Thereafter. They were either dispensed in complete or STS medium. 40 µL of the organoid suspension was plated in each well of a 384 well plate and treated with TMX (0.01-55 µM) with 4 replicates for each concentration. DMSO concentrations never exceeded 1%. Five days later, viability was detected by CellTiterGlow 3D reagent (Promega, cat. no. G9681) according to the manufaturer's indtructions. Cell viability was normalized based on the signal obtained in organoids treated with 1 µM staurosporin (Sigma Aldrich; positive control; corresponding to 0% cell viability) and DMSO (negative control, corresponding to100% viability).

Retroviral and lentiviral transduction

pBABE-puro (PBP), PBP-myr-AKT, pMKO-GFP-shRNA, pMKO-PTEN-shRNA the and lentiviral packaging plasmid (pCMV-dR8.2 dvpr and pCMV-VSV-G) were purchased from Addgene (Cambridge, MA, USA). pLKO and pLKO-EGR1-shRNA1-3 were purchased from Sigma Aldrich S.r.l. (Milan, Italy). For retroviral transduction, 10^6 Phoenix cells were plated in 60mm Petri dishes and allowed to adhere for 24h. Thereafter, cells were transfected with 4µg of plasmid DNA using TransIT-293 (Mirus Bio, Madison, WI) according to the manufacturer's instructions. For lentiviral transduction,10^6 HEK293T cells were plated in 60mm Petri dishes and allowed to adhere for 24h. Thereafter, cells were transfected with 1µg of plasmid DNA, 900ng pCMV-dR8.2 dvpr and 100ng

pCMV-VSV-G using TransIT-293 according to the manufacturer's instructions. Viral supernatants were harvested after 36, 48, 60 and 72h and used to infect MCF7 cells (5×10^5), T47D (6×10^5) cells and ZR-75-1 cells (7×10^5) in 100 mm Petri dishes in the presence of 5 µg/ml protamine sulfate. Successfully infected cells were selected using 1µg/ml puromycin (MCF7) or 1.5 µg/ml puromycin (T47D and ZR-75-1).

Immunoblotting

For protein lysate generation from cultured cells, 5x104 MCF7, T47D or ZR-75-1 cells were plated in 6-well plates in CTR medium. After 24h medium was removed, cells were washed with PBS and incubated either in CTR (10% FCS and 1g/L glucose) or STS (1% FBS, 0,5g/L glucose) medium. After 24h cells were stimulated w/ or w/o with TMX (5 µM) or FULV (10 µM). 24h later, cells were washed twice with cold PBS and then manually scraped in the presence of 50-200 µl lysis buffer (25mM Tris-phosphate, pH 7.8; 2mM DTT; 2mM 1,2-diaminocyclohexane-N,N,N´,N´-tetraacetic acid; 10% glycerol; 1% Triton X-100). Cell lysates were incubated for 15 min on ice, and vortexed for 10 sec every five min. Finally, lysates were spun down at 10.000 g for 2 min at 4°C. Supernatants were recovered and either used immediately or stored at -80°C for subsequent use. Protein lysates from primary tumours or mouse *uteri* were obtained by mechanically homogenizing the tumours or the *uteri* using a mortar and a pestle in cold PBS supplemented with anti-protease and anti-phosphatase cocktails. After homogenization samples were washed twice in cold PBS and the pellets were used for lysate preparation. Protein concentration was determined according to standard Bradford assay. Proteins (35µg) were separated by SDS-PAGE, transferred to a PVDF membrane (Immobilon-P, Millipore S.p.A., Vimodrone, Italy), and detected with the following antibodies: anti-phospho-AKT (Ser473) (#4058, Cell Signaling Technology, Danvers, MA, USA), anti-AKT (#9272, Cell Signaling Technology), anti-PTEN (#9552, Cell Signaling Technology), anti-phospho-p70 S6kinase (Thr389) (#9206, Cell Signaling Technology), anti-p70 S6kinase (#9202, Cell Signaling Technology), , anti-non-phospho-4E-BP1 (#4923, Cell Signaling Technology), anti-phospho-eIF4E (Ser209) (#9741, Cell Signaling Technology), anti-phospho-AMPK (Thr172) (PA5-17831, Thermo Fisher), anti-AMPK (PA5-29679, Thermo Fisher), anti EGR1 (MA5-15008, Thermo Fisher), anti-phospho-Rb (Ser807/811) (#9308, Cell Signaling Technology), anti-Rb (#9309, Cell Signaling Technology), anti CCND1 (#2978, Cell Signaling Technology), , and anti-β-actin (Santa Cruz Biotechnology). Band intensities were quantified by Quantity One SW software (Bio-Rad Laboratories, Inc.) using standard enhanced chemiluminescence.

Colony formation assays

$8x10^2$ MCF7 cells were plated in 6-well plates in regular medium. 24h later cell medium was removed. Cells were washed twice with PBS and were incubated either in CTR or STS medium. The next day cells were treated with either vehicle DMSO, 5 µM TMX or 30 µM fulvestrant for 24h. Then cell medium was removed and cells were cultured for two weeks in regular culture medium before plates were fixed with cold 3% trichloroacetic acid at 4°C for 30 min, washed with cold water and dried overnight. Finally, the plates were stained with 0.4% sulforodhamine B (SRB) in 1% acetic acid, washed four times with 1% acetic acid to remove unbound dye, dried overnight and colonies were counted.

Cell cycle analysis by flow cytometry

MCF7 cells (5×10^5), T47D (6×10^5) cells and ZR-75-1 cells (7×10^5) were plated in 100 mm Petri dishes. 24h later cell medium was removed, cells were washed twice with PBS and were incubated either in CTR or STS medium. The day after cells were treated w/ or w/o TMX (5 µM) or FULV (10 µM) for 72h. Then, cells were resuspended in a buffer containing 0.1% Na citrate, 0.1% Triton-X, and 50 µg/ml propodium iodide. The isolated cell nuclei were analyzed by flow cytometry using a FACS Calibur (Becton Dickinson, Milan, Italy).

Protein Synthesis Assay

$7.5x10^3$ MCF7, 1x104 T47D or ZR-75-1 cells were plated in 96-well plates in CTR medium. After 24h the cell medium was removed, cells were washed with PBS and then incubated either in CTR or STS medium. 24h later cells were stimulated w/ or w/o TMX (5 µM) or FULV (10 µM). Protein synthesis was determined with Click-iT™ Plus OPP Alexa Fluor™ 488 Protein Synthesis Assay Kit

(Life Technologies) according to the manufacturer's guidelines after 24h of treatment. As positive control for the specificity of OPP staining, MCF7 cells were treated with cycloheximide (CHX, Sigma, 10 µM, 1h at 37°C). Cells were analysed with PerkinElmer Operetta® High Content Imaging System.

Luciferase reporter assay

For ER luciferase reporter assays, 4×10^4 MCF7 cells were seeded in a 24-well plate 48h before transfection. Cells were grown in phenol red free regular medium, supplemented with 10% charcoal stripped FBS (Gibco). Cell medium was then replaced and substituted with either regular or STS phenol red free medium, containing 10% or 1% charcoal treated FBS respectively, and 70% confluent cells were transfected with TransIT®-LT1 Transfection Reagent (Mirus). 350 ng of pGL3 promoter plasmid (Promega) or of the pS2/TFF1 reporter vector containing 1.3 kb of the proximal promoter of the estrogen-responsive gene TFF1 cloned in the pGL3-basic backbone[33] were used together with 150ng of the pRLSV40 plasmid (Promega), which harbours the luciferase gene from Renilla reniformis under a constitutive promoter. The next day, transfected cells were treated with tamoxifen (5 µM) or fulvestrant (10 µM) and harvested after additional 24h. Luciferase signals were measured using the Dual-Luciferase® Reporter Assay System (Promega) according to manufacturer's protocol. The firefly luciferase activity was normalized to Renilla luciferase signal, used as normalizer for transfection efficiency. Values are expressed as fold change in comparison to cells transfected with the pGL3 promoter plasmid.

Gene expression profiles and functional analyses

For gene expression microarray studies of cultured MCF7 cells, $5x10^4$ cells were plated in 6-well plates in CTR medium. After 24h medium was removed, cells were washed with PBS and incubated either in CTR (10% FCS and 1g/L glucose) or STS (1% FBS, 0,5g/L glucose) medium. After 24h, cells were stimulated w/ or w/o with 5 µMTMX at the indicated concentrations. 24h later, total RNA isolation was performed with the RNeasy Mini Kit (Quiagen, GmbH Hilden, Germany) according to the manufacturer's instructions. RNAs were hybridized in quadruplicate on Agilent Human GE 4x44K V2 Microarray (G2519F-026652) following the manufacturer's protocol. Hybridized microarray slides were scanned with the Agilent DNA Microarray Scanner G2505C at a 5µm resolution with the manufacturer's software (Agilent ScanControl 8.1.3). The scanned TIFF images were analyzed numerically and background-corrected using the Agilent Feature Extraction Software (version 10.7.7.1), according to the Agilent GE1_107_Sep09 standard protocol. The output of Feature Extraction was analysed with the R software environment for statistical computing (http://www.r-project.org/) and the Bioconductor packages (http://www.bioconductor.org/). The arrayQuality Metrics package was used to check the quality of the arrays. Low signal Agilent probes, identified by a repeated "not detected" flag across the majority of the arrays in every condition, were filtered out from the analysis. Signal intensities across arrays were background corrected (Edwards method) and normalized with the quantile normalization method. DEGs were determined adopting a double threshold based on 1) the magnitude of the change (fold change greater than ± 2) the statistical significance of the change, measured with multiple-test-correction adjustedt (p-value less than 0.05) using Limma package. Gene set enrichment analysis was performed using the version implemented in fgsea package, performing 10000 permutations and using as database the REACTOME Pathways dataset (reactome.db package). Box-plots were generated using ggplot2 package and to evaluate the differences between the groups, non-parametric Wilcoxon-test was used. All microarray data are available through the Gene Expression Omnibus database (http://www.ncbi.nlm.nih.gov/geo/) using the accession number GSE121378.

Quantitative real-time PCR (QPCR)

In QPCR experiments, MCF7, T47D and ZR-75-1 cells were treated as described in the previous section (Gene expression profiles and functional analyses). Total RNA was extracted from cells using RNeasy mini kit (Qiagen S.r.l., Milan, Italy) according to the manufacturer's instructions. 1µg RNA was reverse transcribed in a final volume of 50 µl using High Capacity cDNA Reverse Transcription kit (Life Technologies, Monza, Italy). 5 µl of the resulting cDNA were used for qPCR with a 7900 HT Fast Real-Time PCR (Applied Biosystems by Life Technologies, Monza, Italy).

Gene-specific primers were purchased from Sigma-Aldrich or Thermo Fisher and are listed in Extended Data Table 2. mRNA levels were detected using SYBR Green GoTaq® qPCR Master Mix (Promega Italia S.r.l., Milan, Italy) according to the manufacturer's protocol. Gene expression was normalized to housekeeping gene expression (β-Actin). Comparisons in gene expression were calculated using the $2^{-\Delta\Delta Ct}$ method.

ELISAs

Mice whole blood was collected in Eppendorf. It was allowed to coagulate for 2h at RT, centrifuged 20 minutes at 4,000 rpm, then aliquoted into PCR tubes and stored at -80°C until subsequent use. Patients whole blood was collected in Vacuette Serum Clot Tubes, centrifuged 20 minutes at 2100 rpm then aliquoted into small tubes and stored at -80°C until use. All the ELISAs assay to detect murine and human serum level of IGF-1, IGFBP1, IGFBP3, c-peptide, Leptin and adiponectin were purchased from R&D System except for murine c-peptide which was purchased from Alpco.

Animal models

All mouse experiments were performed in accordance with the relevant laws and institutional guidelines for animal care and use established in the Principles of Laboratory Animal Care (directive 86 /609 /EEC), upon approval by the Italian Istituto Superiore di Sanità. NOD SCID-γ mice were utilized in the experiments from Fig.3h,i and from Extended Data Fig.5h. They were derived from in-house colonies at the animal facility of IFOM-IEO (Milan, Italy) and were kept for a maximum of 3 generations. Breeders (from Charles River Laboratories) and experimental animals were maintained under pathogen-free conditions. Six- to eight-week old female athymic Nude-FoxN1 mice (purchased from Envigo) were utilized in the experiments from Fig.1, 2, 4 and from Extended Data Fig.2, 3, 7 at the Animal Facility of the IRCCS Ospedale Policlinico San Martino (Genoa, Italy). These animals were maintained in air-filtered laminar flow cabinets with a 12-hour light cycle and food and water *ad libitum*. Mice were acclimatized for 1 week. To allow MCF7, T47D and ZR-75-1 xenografts growth, the day before cell injection a 17β-estradiol-releasing pellet (Innovative Research of America, Sarasota, FL, USA) was inserted in the intra-scapular subcutaneous region under anesthesia conditions. $5x10^6$ MCF7, $8x10^6$ ZR-75-1, or $5x10^6$ T47D cells were injected s.c. to either one or both flanks of the mouse or $2.5x10^6$ MCF7 were injected orthotopically into the fourth abdominal fat pad. Treatment was initiated when the tumours appeared as established palpable masses (~2 weeks after cell injection). In each experiment, mice were randomly assigned to one arms (with 6-9 mice per treatment arm): control - *ad lib*. diet; treatment (TMX 45 mg/kg/day in peanut oil via oral gavage[34-36]; FULV 150 mg/kg/once a week via s.c. injection[36-38]; PALB 65 mg/kg, in H_2O, oral gavage, three times a week - Mon, Tue and Fri[39-41]; IGF-1 200 ug/kg body weight[42], s.c., twice a day on the days of the FMD; insulin 20 mU/kg body weight[11], s.c., on the days of the FMD; leptin 1 mg/kg body weight[43], s.c., once a day Monday through Friday, including on the days of the FMD; fasting [water only, for 48h every week][44,45]; FMD[22,44] [for 48-96h every week], or combinations of these treatments as indicated. Body weight and tumour volume were recorded two times a week. Tumour volume was calculated using the formula: tumour volume= $(w2 \times W) \times \pi/6$, where "w" and "W" are "minor side" and "major side" (in mm), respectively. In the short-term experiments, mice were sacrificed after three weeks of treatment. Tumour masses were isolated, weighted, divided in two parts and stored in liquid nitrogen for subsequent RNA extraction, or fixed in formalin for histology. For the resistance acquisition experiments mice were treated with weekly FMD cycles, with a one-week break every fifth week, until the masses quadrupled their initial volume, as this was chosen as the criterion for defining resistance acquisition and disease progression. In Fig.3h, left panel (representing mouse progression-free survival), mice deaths, that were unrelated to disease progression, are presented as outreach symbol on the survival curves. In the experiments with TMX-induced endometrial hyperplasia, six to eight-week old female BALB/c mice were acquired from Envigo and randomly assigned to one arms: control - normal diet; TMX 45mg/kg/day; fasting; FMD; or combinations of these treatments. Body weight was recorded daily. After four weeks of treatment mice were sacrificed, uteri and intra-abdominal fat were collected, imaged and weighted. Uteri were divided in two parts and stored in liquid nitrogen for subsequent RNA extraction and in formalin for histological examination.

Fasting and FMD in mice

Animals were fasted for 48h by complete deprivation of food but with free access to water or FMD was administered for 48-96 hours. The FMD that was utilized in our animal studies consists of two different components designated as day 1 diet and day 2–4 diet that were fed in this respective order as described elsewhere[22,44]. The day 1 diet consists of a mix of various low-calorie broth powders, a vegetable medley powder, extra virgin olive oil, and essential fatty acids; day 2–4 diet consist of low-calorie broth powders and glycerol. Day 1 diet contains 7.67 kJ/g (provided at ~50% of normal daily intake; 0.46 kJ/g protein, 2.2 kJ/g carbohydrate, 5.00 kJ/g fat); the day 2–3 diet is identical on all feeding days and contains 1.48 kJ/g (provided at ~10% of normal daily intake; 0.01 kJ/g protein/fat, 1.47 kJ/g carbohydrates). Mice were housed in a clean new cage to reduce coprophagy and residual chow. Body weight was measured immediately before, during and after the FMD. FMD cycles were repeated every 5 or every 7 days in order obtain complete recover of body weight before a new cycle.

Tissue preparation, histology and immunohistochemistry

Tissue samples of uterus and breast gland were formalin fixed for 24 hours, routinely processed and paraffin embedded. From each paraffin block, 4 micron-thick sections were cut in one session and mounted on Superfrost Plus (Thermo Scientific, Braunschweig, Germany) microscope slides. Sections were stained with Haematoxilin & Eosin (H&E) for microscopic evaluation. Furthermore, sections form uterine samples were used for immunohistochemical staining. Immunohistochemical staining was performed manually. Tissue sections were deparaffinized and rehydrated. Endogenous peroxidase was blocked with 5% H2O2 for 10 minutes. Heat pre-treatment was carried out by Microwave (3 minutes at 900 watt plus 13 minutes at 360 watt) in a citrate buffer at pH6. Polyclonal antibody for Ki67 (Cell Signaling, D2H10) diluted 1:50 plus Dako EnVision^{extended} and Dual Link System HRP coupled with DAB detection kit were used for Ki67 staining. After immunostaining slides were counterstained with haematoxylin and coverslipped.
Concerning histological and immunohistochemical evaluation, all stains and immunostains were evaluated by one expert pathologist (LM) blinded as to different treatments. Mammary gland samples from mice treated with TMX were analysed qualitatively to evaluate the epithelial component and any (cytological and architectural) deviance from normality when present.

Clinical studies of FMDs in patients undergoing ET for HR+ BC

The NCT03595540 was conducted at the IRCCS Ospedale Policlinico San Martino (Genoa, Italy). This trial consist of a single-arm phase II clinical study of a FMD (Prolon, by L-Nutra, Los Angeles, CA) in 60 patients with solid or hematologic tumours undergoing treatment with chemotherapeutic regimens, hormone therapies, other molecularly targeted therapies (including kinase inhibitors), biological drugs (including trastuzumab, pertuzumab, cetuximab and bevacizumab) or inhibitors of immune checkpoints (e.g. Opdivo, Keytruda). An amendment to the protocol (which includes the possibility of using imaging studies that are otherwise routinetly prescribed for disease monitoring, e.g. CT scans, for body composition evaluation) was approved by the Ethics Committee of the Regione Liguria on April 8th 2019 (#27). The FMD tested, Prolon (L-Nutra, Los Angeles, CA) is a FMD lasting five days, whose composition was described elsewhere[22,23]. In brief, it consists of vegetable soups, broths, bars, olives, crackers, herbal teas, supplements of vitamins and minerals. Day 1 of the FMD supplies ~4600 kJ (11% protein, 46% fat, and 43% carbohydrate), whereas days 2-to-5 provide ~3000 kJ (9% protein, 44% fat, and 47% carbohydrate) per day. Throughout the clinical study, patients have received rigorous clinical and nutritional follow-up along with dietary counseling for the intervals between FMD cycles, aiming at providing an appropriate intake of proteins (1.5 g/kg ideal weight/day, primarily from seafood and legumes), essential fatty acids, vitamins and minerals[24,25] and have also been invited to perform light/moderate daily muscle training (e.g. 500-600 kJ/day; as allowed by their medical condition; https://docs.google.com/presentation/d/1szaRW4t-pZQI17o2Pe0747FsUEOVWWiA6BHja0p8H_0/edit#slide=id.g34ad797184_0_0) to enhance muscle anabolism[46]. Patients have received reduced FMD cycles (only the first 3 or the first 4 days of the FMD kit) when a reduction in body weight or in phase angle exceeding 10% of the baseline value was detected or for phase angle values decreasing below 5.2 degrees. The FMD cycle was not administered whenever the phase angle value was found to be below 5 degrees. Between FMD

cycles patients were prescribed amino acid supplements (Aminotrofic; 30 g essential amino acids two times a day) in the presence of a difficulty in maintaining phase angle values of 5 degrees or greater. Primary endpoints of the study are the feasibility and safety of monthly cycles of the FMD in patients with solid or hematologic tumours who undergo active treatment. Feasibility was defined as the strict adherence to the diet prescribed in all its days with the possibility of admitting the consumption of only 50% of the planned diet or a maximum consumption of 4-5 Kcal kg body weight of food not provided in only one of the five days of each cycle. It has been monitored by food diary and/or phone calls during the FMD days. FMD-emergent side effects are monitored according to the NCI-CTCAE version 5.0. Secondary endpoints include: i) patient nutritional status as monitored by weight, handgrip strength and bio-impedance; ii) quality of life (QLQ-C30); iii) clinical responses measured by CT, MRI or by dosing of tumour markers and / or molecular biology tests; effect of FMD on circulating levels of IGF-1 and other factors. Inclusion criteria are: written informed consent; age > 18 years; patients with solid or hematologic tumours undergoing active treatment; ECOG performance status 0-1; adequate organ function; BMI >21 kg/m2 (with possibility to also enroll patients with a BMI between 19 and 21 kg/m^2 based on the judgement of the treating physician); low nutritional risk according to nutritional risk screening (NRS). Exclusion criteria are diabetes mellitus; previous therapy with IGF-1 inhibitors; food allergies to the components of the FMD; BMI <19 kg/m^2; bio-impedance phase angle <5.0 degrees; medium/high nutritional risk according to NRS; any metabolic disorder that can affect gluconeogenesis or ability to adapt to fasting periods; patients who live alone or are not adequately supported by the family context; treatment in progress with other experimental therapies. Patient serum for subsequent ELISA assays of circulating growth factors and adipokines has been routinely collected before commencement of the first and of the second FMD cycle. In addition, in those patients who live close to the enrolment site, blood draws were also performed on day 6 of the FMD at cycle. Blood glucose and ketone bodies were self-measured by the patients using Glucomen Areo 2k (Menarini, Italy).

The NCT03340935 clinical trial, was conducted at the Fondazione IRCCS Istituto Nazionale dei Tumori, Milan, Italy. This study aimed to assess the safety, feasibility and metabolic effects of a FMD in cancer patients treated with different standard antitumor therapies. Patients with any malignancy, with the exception of small cell neuroendocrine tumors, were considered for enrollment in this study. The FMD was administered up to a maximum of 8 consecutive cycles in combination with standard adjuvant treatments or therapies for advanced disease. The FMD utilized in this stufdy consisted of a 5-day plant-based, low-calorie (600 Kcal on day 1, followed by 300 KCal/day on days 2 to 5), low-protein, low carbohydrate diet. Primary study endpoint was safety of the FMD in cancer patients (graded according to the NCI CTCAE v 4.03). Secondary outcome measures include i) feasibility of the FMD in cancer patients (defined as the ability of the patient to comply with the prescribed dietary regimen, as assessed through the analysis of food diaries filled by patients during the five days of each FMD cycle); ii) metabolic effects of the FMD; iii) effects of the FMD on blood growth factors; iv) weight changes during the FMD; v) changes in blood cell counts; vi) changes in kidney function parameters; vii) FMD-induced changes in parameters linked to kidney function, such as blood urea nitrogen, creatinine and uric acid; viii) FMD-induced changes in parameters linked to liver function, such as aspartate and alanine transaminases, total bilirubin. Inclusion criteria were cytologically or histologically confirmed diagnosis of malignant neoplasm; capability of swallowing plant-based foods foreseen by the FMD; body mass index (BMI) ≥ 20 kg/m2; adequate bone marrow function; creatinine < 1.5 mg/dl or calculated creatinine clearance ≥50 mL/min; uric acid < 6 mg/dl; fasting glucose > 65 mg/dl; total bilirubin < 2 mg/dl or < ULN, except for patients with Gilbert syndrome; written informed consent; willingness and ability to accomplish blood and urinary examinations according to the protocol; ability to maintain a daily contact (by phone or email) with the study staff for the communication of crucial clinical information, including daily body weight, blood pressure, health status and adverse events during each of the 5 days on diet. Exclusion criteria were small cell neuroendocrine carcinoma; unintentional weight loss ≥ 5% in the last 3-6 months; known HIV infection; pregnancy or lactation;history of alcohol abuse; diagnosis of diabetes mellitus type I or type II that requires medical treatment; fasting glucose > 200 mg/dl; clinically meaningful cardiovascular, renal or pulmonary diseases; current treatment with antipsychotics.

CT scan-based body composition analysis

CT scans of Pt.#1 and Pt.#3 were acquired with different CT scanners. Both 1.25-mm and 5-mm slice thickness with standard body kernel were available. All CT scans were performed with the patient in the supine position, head first on the scanner table and with the arms raised and placed behind the patient's head, out of the scan plane. The whole body was scanned from the lung apex to the pubic symphysis (Pt.#1). To assess measurement reproducibility, a strict method was used as follows to guarantee an intra-reader agreement of the experienced reader (A.T., radiologist with more than 10 years of experience in oncological imaging) of 0.98 and 0.94 for 1.25-mm and 5-mm, respectively[47]. Reconstructed axial images with both a 1.25-mm and a 5-mm slice thickness were analysed using the software installed on the workstations of the IRCCS Ospedale Policlinico San Martino Radiology Department (Suite-Estensa 1.9-Ebit-Esaote Group Company, 2015). The third lumbar vertebra (L3), at the level in which both transverse processes are clearly visible, was the bony landmark for the estimation of total muscle area and subcutaneous fat. If abdominal CT scans were not available, but only thoracic CT was present (Pt.#3), estimation of total muscle area (red areas) and fat at the level of the Louis angle (manubriosternal joint that lies at the level of the second costal cartilage) at baseline and after repeated FMD cycles were done according to[47].

Statistical Analysis

All in vitro data are represented as mean ± SD of at least three independent experiments. All in vivo data are represented as mean ± SEM. Statistical analyses were performed with GraphPad Prism software version 5 (GraphPad Software). All parameters were tested by paired t test or one-way ANOVA followed by Tukey's test. p values <0.05 were considered significant. To evaluate changes in fat-free body mass, fat body mass and phase angle over time, we fitted a linear mixed effects model taking into account absolute (values expressed as kgs) fat-free body mass, absolute fat body mass (values expressed as kgs) and phase angle (values expressed as degrees) as a function of time assessment, with a random covariate represented by subject ID (package lme4 in the R Environment for Statistical Computation).

Acknowledgments This work was supported in part by the Associazione Italiana per la Ricerca sul Cancro (AIRC) (IG#17736 and #22098 to A.N.; IG#17605 to V.D.L. and MFAG#22977 to C.V.), the Fondazione Umberto Veronesi (to A.N.), the Italian Ministry of Health (GR-2011-02347192 to A.N.), the 5 × 1000 2014 Funds to the IRCCS Ospedale Policlinico San Martino (to A.N.), the BC161452 and BC161452P1 grants of the Breast Cancer Research Program (US Department of Defense) (to V.D.L. and to A.N., respectively) and the US National Institute on Aging-National Institutes of Health (NIA–NIH) grants AG034906 and AG20642 (to V.D.L.). The authors would like to thank the High Throughput Screening Facility of the University of Trento (Italy) for their technical support, and Prof. Alberto Ballestrero and Prof. Lucia Del Mastro (Department of Internal Medicine and Medical Specialties, University of Genoa) for the helpful discussion.

Author contribution A.N. and V.D.L. conceived the study. I.C., V.S., P.B., M.W., S.B., C.Z., E.D., L.M., M.C., V.G.V., F.P., M.P., G.S., S.C. performed all experiments. S.P., G.Z., and L.F. performed computational and statistical analyses. F.V., C.V., A.L.C., R.G., C.M., S.S., A.T., A.A. participated in the clinical trials, collected and analysed clinical data. M.C., P.O., F. M., H.C., F.D.B. and A.P. contributed to the study design, advised on model building and analysed data. All authors evaluated the results and edited the manuscript. A.N. and V.D.L. wrote the manuscript with input from all authors.

Competing interest A.N. and I.C. hold intellectual property rights on uses of fasting-mimicking diets in cancer. V.D.L. has equities in L-Nutra.

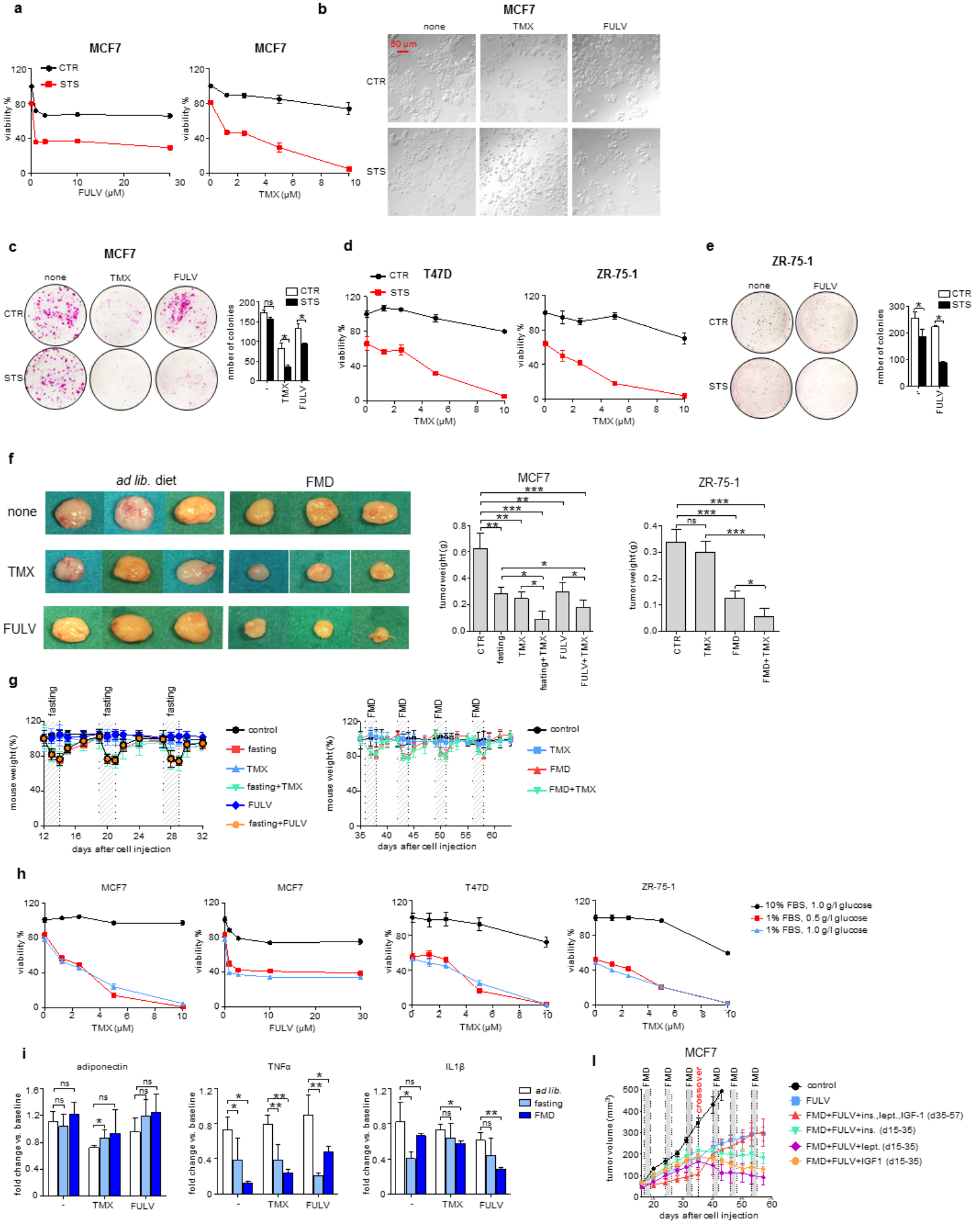
a
MCF7
CTR
STS
viability %
FULV (μM)
MCF7
TMX (μM)
b
MCF7
none
TMX
FULV
50 μm
CTR
STS
c
MCF7
none
TMX
FULV
CTR
STS
nmber of colonies
ns
d
T47D
ZR-75-1
CTR
STS
viability %
TMX (μM)
e
ZR-75-1
none
FULV
CTR
STS
nmber of colonies
f
ad lib. diet
FMD
none
TMX
FULV
MCF7
ZR-75-1
tumor weight (g)
CTR
fasting
TMX
fasting+TMX
FULV
FULV+TMX
FMD
FMD+TMX
g
fasting
mouse weight (%)
days after cell injection
control
fasting
TMX
fasting+TMX
FULV
fasting+FULV
FMD
FMD+TMX
h
MCF7
MCF7
T47D
ZR-75-1
viability %
TMX (μM)
FULV (μM)
10% FBS, 1.0 g/l glucose
1% FBS, 0.5 g/l glucose
1% FBS, 1.0 g/l glucose
i
adiponectin
TNFα
IL1β
fold change vs. baseline
ad lib.
fasting
FMD
l
MCF7
tumor volume (mm³)
crossover
days after cell injection
control
FULV
FMD+FULV+ins.,lept.,IGF-1 (d35-57)
FMD+FULV+ins. (d15-35)
FMD+FULV+lept. (d15-35)
FMD+FULV+IGF1 (d15-35)

Extended Data Fig. 1. Fasting/FMD enhance ET antitumor activity in HR+ BC. a-e, Viability and colony formation assays in MCF7, T47D and ZR-75-1 cells reated w/ or w/o ETs and STS-conditions. f, MCF7 or ZR-75-1 xenografts masses were excised from BALB/c athymic mice (nu+/nu+) treated for three weeks with TMX, FULV, weekly 48h FMD or combined ET and FMD, imaged (left, MCF7) and weighted (right). g, Mouse weight during treatment with TMX/FULV, fasting/FMD or their combinations in MCF7 xenograft- or ZR-75-1 xenograft-bearing mice. H, Effect of glucose add-back in HR+ BC cells treated with TMX, FULV, STS-conditions and their combination. a, Serum adiponectin, Tnf and Il1β concentration (fold change vs. baseline) in six- to eight-week-old BALB/c athymic mice (nu+/nu+) before and after a 48h fasting/FMD (or *ad lib*. diet) w/ or w/o concomitant treatment. TMX/FULV. h, i, MCF7 xenograft growth in six- to eight-week-old BALB/c athymic mice (nu+/nu+) treated w/ or w/o FULV, FULV plus weekly FMD, or combination of FULV, weekly FMD and i.p. insulin, IGF-1, leptin, or the three FRFs combined. At day 35 (crossover), FRFs administration was withdrawn, while it was started in mice that had only received FULV plus FMD.

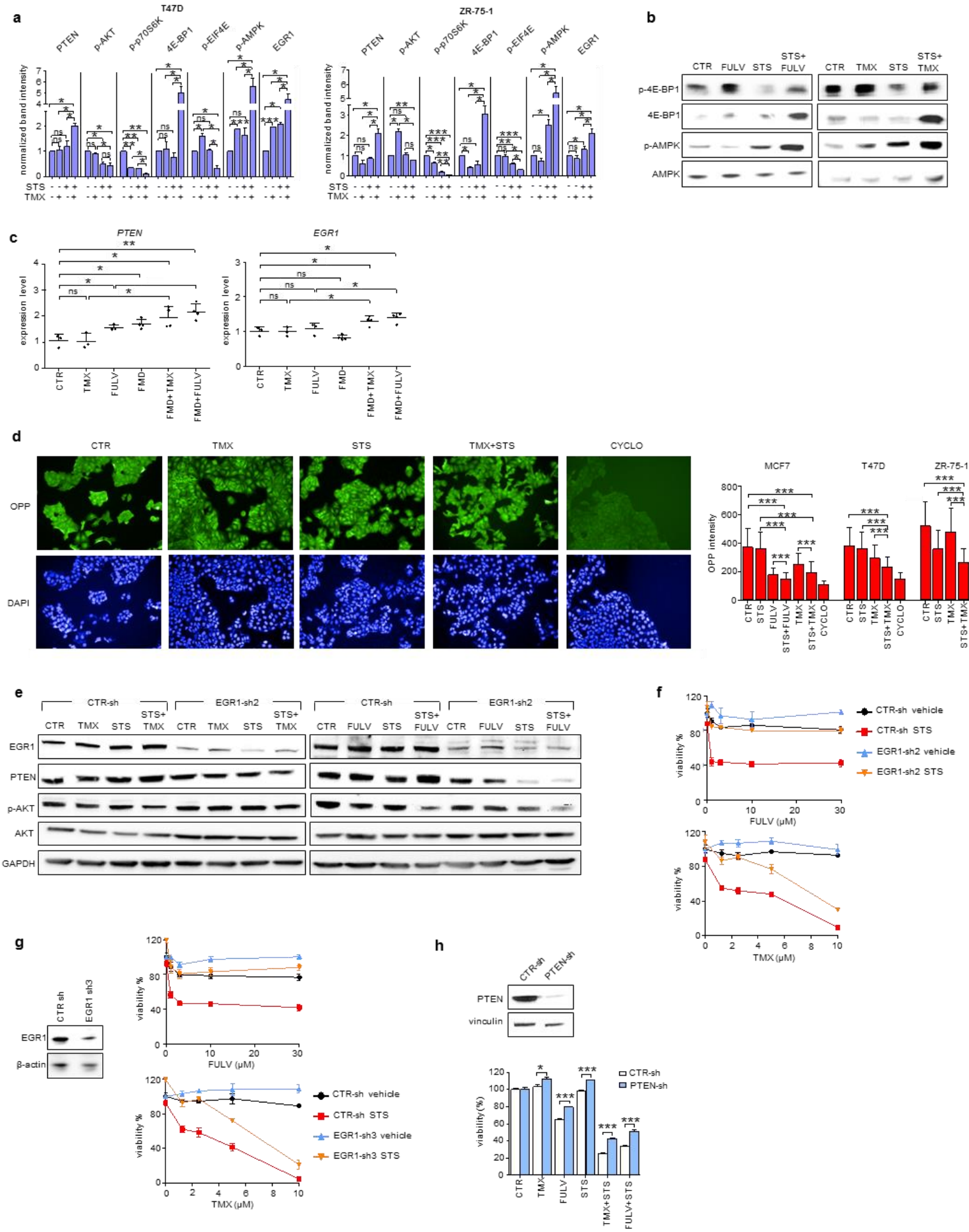
a
T47D
ZR-75-1
PTEN
p-AKT
p-p70S6K
4E-BP1
p-EIF4E
p-AMPK
EGR1
normalized band intensity
STS
TMX
b
CTR
FULV
STS
STS+ FULV
TMX
STS+ TMX
p-4E-BP1
4E-BP1
p-AMPK
AMPK
c
PTEN
EGR1
expression level
CTR
TMX
FULV
FMD
FMD+TMX
FMD+FULV
d
CTR
TMX
STS
TMX+STS
CYCLO
OPP
DAPI
MCF7
T47D
ZR-75-1
OPP intensity
e
CTR-sh
EGR1-sh2
EGR1
PTEN
p-AKT
AKT
GAPDH
f
CTR-sh vehicle
CTR-sh STS
EGR1-sh2 vehicle
EGR1-sh2 STS
viability %
FULV (μM)
TMX (μM)
g
CTR sh
EGR1 sh3
EGR1
β-actin
CTR-sh vehicle
CTR-sh STS
EGR1-sh3 vehicle
EGR1-sh3 STS
h
CTR-sh
PTEN-sh
PTEN
vinculin
viability(%)

Extended Data Fig. 2. Fasting/FMD and ETs cooperate to inhibit PI3K/AKT/mTOR signaling in HR+ BC cells. a, Normalized protein band intensities for the PI3K/AKT/mTOR signaling cascade in ZR-75-1 and T47D. b, 4EBP1 and AMPK phosphorylation in MCF7 treated with TMX, FULV, STS-conditions or their combination. c, PTEN and EGR1 expression level in MCF7-xenograft from BALB/c athymic mice (nu+/nu+) treated with FULV, TMX, FMD or their combinations. d, OPP-based determination of protein synthesis in MCF7, T47D and ZR-75-1 treated with TMX/FULV, STS-conditions and their combinations. e, EGR1, PTEN, GAPDH levels, and AKT phosphorylation in MCF7 cells in response to EGR1 silencing (with EGR1-shRNA#2), TMX, FULV, STS conditions, or their combinations. f, g, Viability of control and of EGR1-silenced MCF7 (EGR1-shRNA#2 and #3) in response to TMX, FULV, STS-conditions, or their combinations; in g, left inset, EGR1 and β-actin levels in control and in EGR1-shRNA#3-expressing MCF7 were detected by Western blotting. h, MCF7 cell viability in response to PTEN silencing, TMX, FULV, STS conditions, or their combination; in the upper inset, PTEN and vinculin levels in control and in PTEN-shRNA-expressing MCF7 were detected by Western blotting.

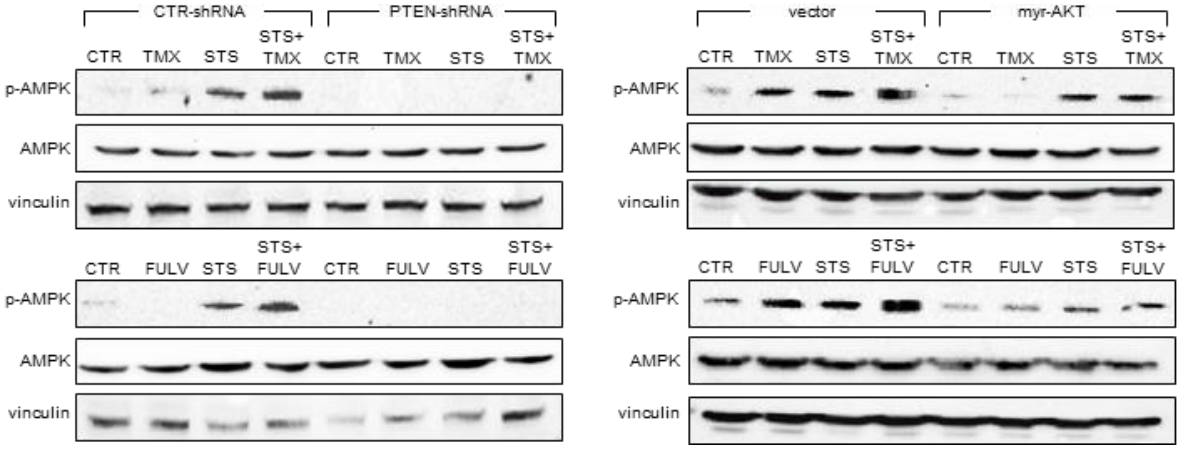

Extended Data Fig. 3. AMPK phosphorylation regulation in response to ET and STS-conditions is dependent on AKT inhibition. AMPK phosphorylation and and vinculin levels in MCF7 with silenced PTEN or overexpressed myr-AKT and treated w/ or w/o TMX/FULV, STS-conditions and their combinations were detected by Western blotting.

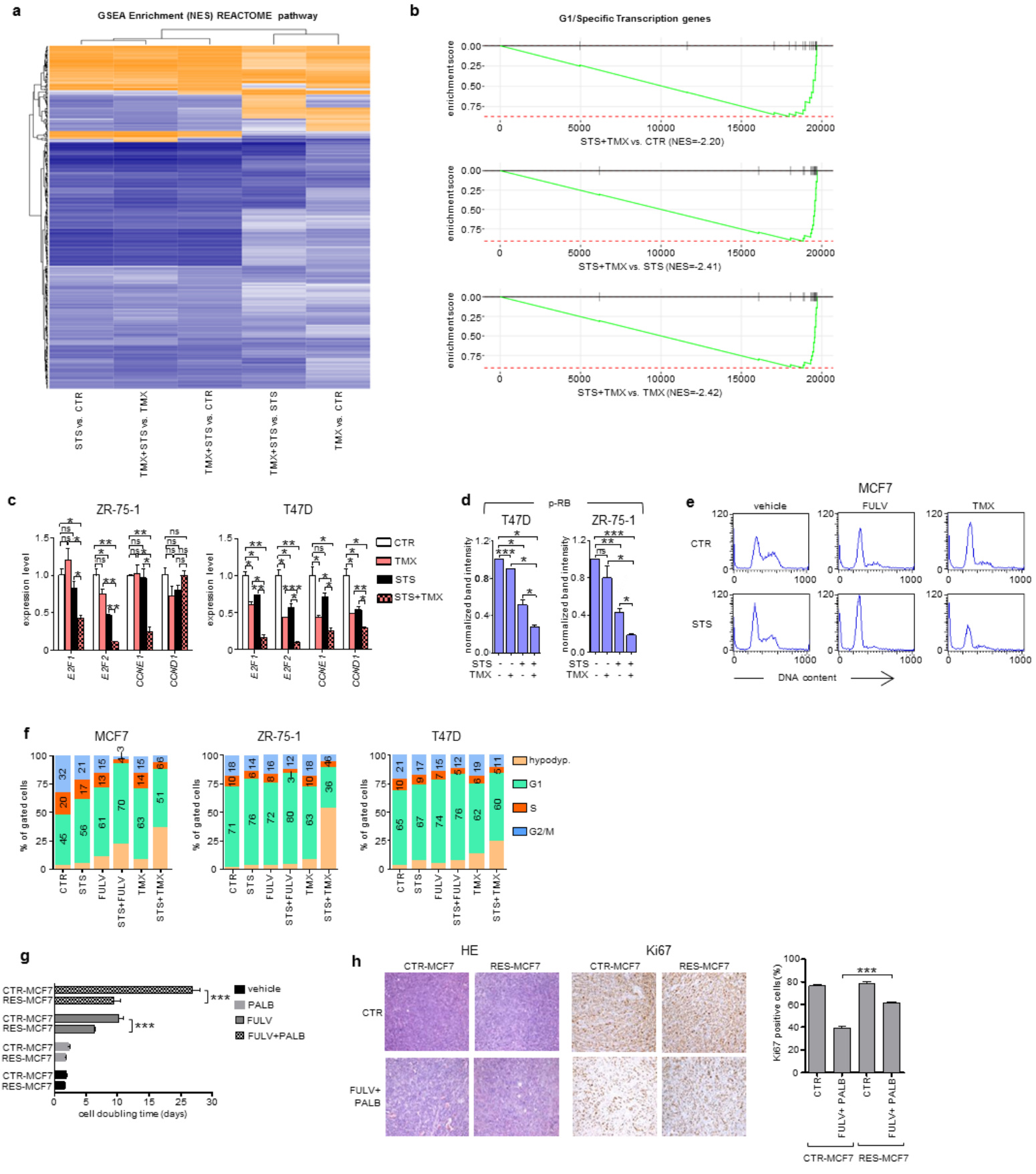

Extended Data Fig. 4. FMD cooperates with ETs to induce cell cycle arrest in HR+ BC. a, b, Gene Set Enrichment analyses of MCF7 treated with TMX, STS and combination. c, d, *E2F1/E2F2/CCND1/CCNE1* mRNA expression and quantification of phosphorylated RB protein in T47D and ZR-75-1 treated with TMX/FULV, STS-conditions and their combinations. e, f, Cell cycle analyses of MCF7/T47D/ZR-75-1 treated w/ or w/o TMX/FULV and STS. g, Doubling time of control MCF or of *ex vivo* cultured MCF7 resistant to FULV plus PALB (RES-MCF7) upon treatment with FULV, STS, palbociclib or their combinations. h, Hematoxylin and eosin (HE) staining and immunohistochemical staining for Ki67 of xenografts of control MCF7 or RES-MCF7 treated w/ or w/o FULV and PALB.

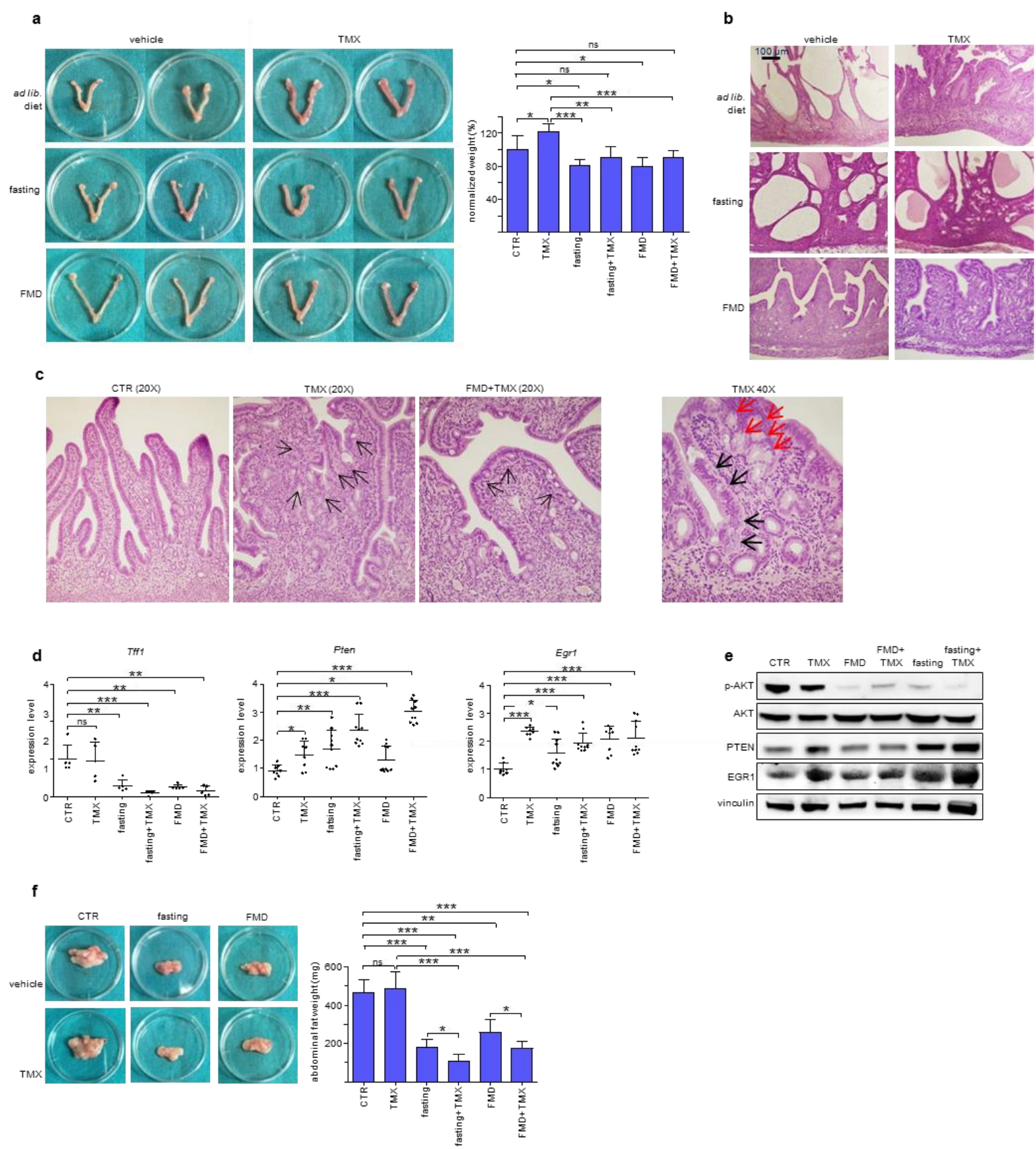
a
vehicle
TMX
ad lib. diet
fasting
FMD
normalized weight (%)
CTR
TMX
fasting
fasting+TMX
FMD
FMD+TMX
b
vehicle
TMX
100 µm
ad lib. diet
fasting
FMD
c
CTR (20X)
TMX (20X)
FMD+TMX (20X)
TMX 40X
d
Tff1
Pten
Egr1
expression level
e
CTR
TMX
FMD
FMD+ TMX
fasting
fasting+ TMX
p-AKT
AKT
PTEN
EGR1
vinculin
f
CTR
fasting
FMD
vehicle
TMX
abdominal fat weight (mg)

Extended Data Fig. 6. Fasting/FMD prevents TMX-induced endometrial hyperplasia and reduce intra-abdominal fat. a, b, Appearance, weight and histology of uteri from BALB/C mice treated with TMX, FMD, water fasting or their combinations for four weeks. c, Left panel: uteri of TMX treated mice show wider and thicker villi and tufts/blebs budding from the epithelium (black arrows). Right panel: TMX induces small blebs of a few cells (black arrows) begin to form from the superficial epithelium and then acquire the lumen and form glands that gradually separate (red arrows). d, effect of TMX, water fasting, FMD and their combinations on Tff1, Pten and Egr1 expression in mouse uteri. e, effect of TMX, water fasting, FMD and their combinations on AKT phosphorylation, PTEN and EGR1 expression in mouse uteri. f, Appearance and weight of the abdominal fat isolated from BALB/C mice treated with TMX, FMD, water fasting or their combinations for four weeks.

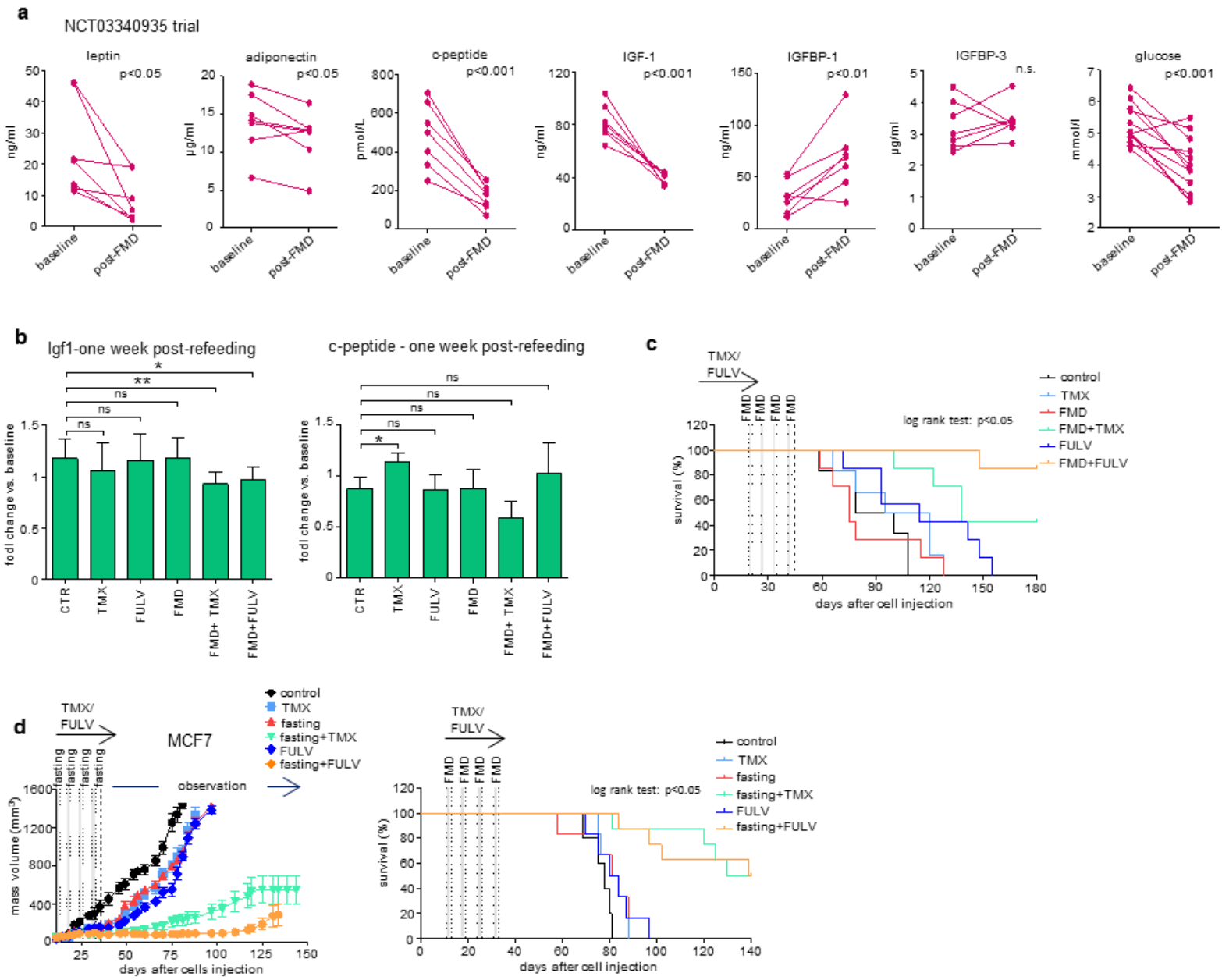

Extended Data Fig. 7. Effects of periodic FMD on circulating growth factors and disease in patients with HR+ BC and mice xenograft. a, serum leptin, adiponectin, c-peptide, IGF-1, IGFBP1 and IFGBP3 before and after a FMD cycle in BC patients treated with ET and FMD in the NCT03340935 trial. b, IGF-1 and c-peptide levels in serum from mice treated with FULV, TMX, weekly FMD or their combination for two weeks, one week after the end of the last FMD cycle. c, MCF7 xenograft PFS after a one-month treatment w/ or w/o TMX, FULV, FMD or their combination. d, MCF7 xenograft growth and PFS after a one-month treatment w/ or w/o TMX, FULV, fasting or their combination followed by observation.

Extended Data Table 1. Patient characteristics, adverse events and best response

Pt. no	Age	BMI at enrollment (kg/m^2)	Stage and HER2 status	type of ET and other therapies	Adjuvant (A) vs. palliative (P) therapy	Site of metastasis	No of FMD cycles	Reduced/non-administered FMD cycles	Adverse events	Best response
1	51	34.4	IV; HER2-neg	FULV+PALB	P	lymph nodes	10	1 reduced cycle (4d)	none	SD
2	46	34.8	IV; HER2-pos	exemestane+trastuzumab; pertuzumab	P	liver, lung, lymph nodes	6	none	diarrhea (G2)	SD
3	62	25.3	IV; HER2-neg	letrozole	P	pleura	13	4 reduced cycles (3-4d) and 1 non-administered cycle	none	SD
4	55	26.4	IIB; HER2-neg	exemestane	A	N/A	4	2 reduced cycles (3-4d)	diarrhea (G2)	NED
5	37	22.1	IA; HER2-neg	Exemestane+leuprorelin	A	N/A	9	1 reduced cycle (4d)	none	NED
6	54	32.3	IIB; HER2-neg	letrozole	A	N/A	12	none	headache (G1); fatigue (G2) hypotension (G2)	NED
7	52	19.6	IV; HER2-neg	exemestane	P	bone	12	1 reduced cycle (4d)	headache (G1)	SD

8	48	22.2	IIB; HER2-neg	exemestane+leuprorelin	A	N/A	12	none	headache (G1); tinnitus (G1)	NED
9	54	25.2	IIA; HER2-neg	exemestane	A	N/A	3	none	headache (G1)	NED
10	54	22.4	IA; HER2-neg	letrozole	A	N/A	5	none	headache (G1)	NED
11	46	22.3	IA; HER2-neg	letrozole+leuprorelin	A	N/A	11	4 reduced cycles (4d)	fatigue (G2); headache(G1)	NED
12	49	23	IIB; HER2-pos	exemestane+trastuzumab+leuprorelin	A	N/A	4	none	none	NED
13	42	26.2	IA; HER2-neg	exemestane+leuprorelin	A	N/A	2	none	none	NED
14	56	22.9	IIB	exemestane	A	N/A	4	none	abdominal pain (G1)	NED
15	43	33.4	IV	FULV+abemaciclib	P	Skin, lung, bone, lymph nodes	1	none	none	SD
16	42	21.9	IIB	exemestane+leuprorelin	A	N/A	4	1 reduced cycle (3d)	none	NED
17	45	30.4	IIB	tamoxifen+leuprorelin	A	N/A	6	none	Fatigue (G1); hypotension (G2); headache (G1)	NED
18	57	25	IV	letrozole	A	N/A	4	none	none	SD
19	44	30.4	IIA	tamoxifen+leuprorelin	A	N/A	4	none	fatigue (G1); headache (G1)	NED

20	50	25.4	IA	tamoxifen+leuprorelin	A	N/A	2	1 reduced cycle (3d); 1 cycle not administered	none	NED
21	58	21.3	IB	letrozole	A	N/A	9	1 reduced cycle (4d)	fatigue (G1)	NED
22	48	42.1	IIB	exemestane+leuprorelin	A	N/A	4	none	none	NED
23	62	27.6	IIIC	exemestane	A	N/A	4	none	headache (G1)	NED
24	50	24.5	IB	exemestane+leuprorelin	A	N/A	1	none	headache (G1), fatigue (G1)	NED
25	67	21.1	IV	exemestane+everolimus	P	bone	2	N/A	fatigue (G2)	PR
26	52	26.44	IV	FULV+PALB	P	Bone	8	N/A	Fatigue (G2), headache (G1)	CR
27	50	21.77	IV	FULV+PALB+triptorelin	P	Bone, liver	8	N/A	fatigue (G2), headache (G1), vomiting (G1)	CR
28	53	23.84	IV	FULV	P	Bone, liver, lymph nodes	4	N/A	Fatigue (G3), vomiting (G2), rash (G1)	SD
29	52	23.98	IV	FULV+PALB	P	Lung, liver, bone, lymph nodes	5	N/A	Fatigue (G1), nausea (G1), vomiting (G1), tachycardia (G1)	SD
30	50	23.16	IV	tamoxifen	P	Lung, bone, lymph nodes	5	N/A	Fatigue (G1), headache (G1)	SD
31	43	21.72	IV	FULV+leuprorelin	P	Bone	2	N/A	Fatigue (G1), nausea (G1), dizziness (G1), vomiting (G1), headache (G1)	PD

32	44	29.4	IA	tamoxifen+triptorelin	A	N/A	8	N/A	Fatigue (G2), nausea (G1), headache (G1), vomiting (G1)	NED
33	61	33.12	IIB	letrozole	A	N/A	5	N/A	Fatigue G2	NED
34	50	26.9	IIB	tamoxifen	A	N/A	8	N/A	Fatigue (G2), constipation (G1), hot flushes (G1)	NED
35	73	20.82	IA	letrozole	A	N/A	7	N/A	Nausea (G1), fatigue (G1), headache (G1)	N/A
36	55	21.13	IIA	letrozole	A	N/A	4	N/A	Fatigue (G1), headache (G1), dizziness (G1), muscle cramps (G1)	N/A

Legend to Extended Data Table 1: CR: complete response; PR: partial response; SD: stable disease; NED no evidence of disease; Pts. 1-24 are from trial NCT…; Pts. 25-36 are from trial NCT03340935.

Extended Data Table 2. Complete blood counts and metabolic panel post-FMD (within 48h from the end of a FMD cycle) in BC patients

	Pt.#3	Pt.#6	Pt.#7	Pt.#...	Pt.#---
RBC					
Hemoglobin (g/dl; …-….)					
MCV					
WBC					
Plt					

Legend to Extended Data Table 2: … .

Extended Data Table 3. Primer list

Human ACTB	FW	CGGGAAATCGTGCGTGACATTAAG
	REV	TGATCTCCTTCTGCATCCTGTCGG
Human TFF1	FW	TTTGGAGCAGAGAGGAGGCAATG
	REV	ACCACAATTCTGTCTTTCACGGGG
Human E2F1	FW	ATGTTTTCCTGTGCCCTGAG
	REV	ATCTGTGGTGAGGGATGAGG
Human E2F2	FW	CTCTCTGAGCTTCAAGCACCTG
	REV	CTTGACGGCAATCACTGTCTGC
Human CCNE1	FW	TGTGTCCTGGATGTTGACTGCC
	REV	CTCTATGTCGCACCACTGATACC
Human CCND1	FW	GCCTCTAAGATGAAGGAGAC
	REV	CCATTTGCAGCAGCTC
Human EGR1	FW	GCAGAGTCTTTTCCTGAC
	REV	TTGGTCATGCTCACTAGG
Human PTEN	FW	GGCTAAGTGAAGATGACAA
	REV	GTTACTCCCTTTTTGTCTCT
Human TFF1	FW	TTTGGAGCAGAGAGGAGGCAATG
	REV	ACCACAATTCTGTCTTTCACGGGG
Human GREB	FW	CTTGGTTTCTCTGGGAATTG
	REV	TTCCAACAGATTAAAGGTCC
mouse Actb	FW	GATGTATGAAGGCTTTGGTC
	REV	TGTGCACTTTTATTGGTCTC
mouse Egr1	FW	CAGAGTCCTTTTCTGACATC
	REV	GAGAAGCGGCCAGTATAG
mouse Pten	FW	AACTTGCAATCCTCAGTTTG
	REV	CTACTTTGATATCACCACACAC
mouse Tff1	FW	CTCAAGAAGAAGAATGTCCC
	REV	CTCTTTTAATTCTCAGGCCG

1 DeVita, V. J., Laurence, TS. , Rosenberg, SA. . *DeVita, Hellmann and Rosenberg's cancer: principles & practice of oncology*. 11th edn, 1269-1316 (Wolters Kluwer, 2019).

2 Ferlay, J. *et al.* Cancer incidence and mortality worldwide: sources, methods and major patterns in GLOBOCAN 2012. *International journal of cancer* **136**, E359-386, doi:10.1002/ijc.29210 (2015).

3 Araki, K. & Miyoshi, Y. Mechanism of resistance to endocrine therapy in breast cancer: the important role of PI3K/Akt/mTOR in estrogen receptor-positive, HER2-negative breast cancer. *Breast cancer* **25**, 392-401, doi:10.1007/s12282-017-0812-x (2018).

4 AlFakeeh, A. & Brezden-Masley, C. Overcoming endocrine resistance in hormone receptor-positive breast cancer. *Current oncology* **25**, S18-S27, doi:10.3747/co.25.3752 (2018).

5 Lee, A. V., Cui, X. & Oesterreich, S. Cross-talk among estrogen receptor, epidermal growth factor, and insulin-like growth factor signaling in breast cancer. *Clinical cancer research : an official journal of the American Association for Cancer Research* **7**, 4429s-4435s; discussion 4411s-4412s (2001).

6 Sachs, N. *et al.* A Living Biobank of Breast Cancer Organoids Captures Disease Heterogeneity. *Cell* **172**, 373-386 e310, doi:10.1016/j.cell.2017.11.010 (2018).

7 Jones, J. I. & Clemmons, D. R. Insulin-like growth factors and their binding proteins: biological actions. *Endocrine reviews* **16**, 3-34, doi:10.1210/edrv-16-1-3 (1995).

8 Sanchez-Jimenez, F., Perez-Perez, A., de la Cruz-Merino, L. & Sanchez-Margalet, V. Obesity and Breast Cancer: Role of Leptin. *Frontiers in oncology* **9**, 596, doi:10.3389/fonc.2019.00596 (2019).

9 Garofalo, C., Sisci, D. & Surmacz, E. Leptin interferes with the effects of the antiestrogen ICI 182,780 in MCF-7 breast cancer cells. *Clinical cancer research : an official journal of the American Association for Cancer Research* **10**, 6466-6475, doi:10.1158/1078-0432.CCR-04-0203 (2004).

10 Bougaret, L. *et al.* Adipocyte/breast cancer cell crosstalk in obesity interferes with the anti-proliferative efficacy of tamoxifen. *PloS one* **13**, e0191571, doi:10.1371/journal.pone.0191571 (2018).

11 Hopkins, B. D. *et al.* Suppression of insulin feedback enhances the efficacy of PI3K inhibitors. *Nature* **560**, 499-503, doi:10.1038/s41586-018-0343-4 (2018).

12 Pollak, M. The insulin and insulin-like growth factor receptor family in neoplasia: an update. *Nature reviews. Cancer* **12**, 159-169, doi:10.1038/nrc3215 (2012).

13 Jarde, T., Perrier, S., Vasson, M. P. & Caldefie-Chezet, F. Molecular mechanisms of leptin and adiponectin in breast cancer. *European journal of cancer* **47**, 33-43, doi:10.1016/j.ejca.2010.09.005 (2011).

14 Saxena, N. K. *et al.* Concomitant activation of the JAK/STAT, PI3K/AKT, and ERK signaling is involved in leptin-mediated promotion of invasion and migration of hepatocellular carcinoma cells. *Cancer research* **67**, 2497-2507, doi:10.1158/0008-5472.CAN-06-3075 (2007).

15 Cristofanilli, M. *et al.* Fulvestrant plus palbociclib versus fulvestrant plus placebo for treatment of hormone-receptor-positive, HER2-negative metastatic breast cancer that progressed on previous endocrine therapy (PALOMA-3): final analysis of the multicentre, double-blind, phase 3 randomised controlled trial. *The Lancet. Oncology* **17**, 425-439, doi:10.1016/S1470-2045(15)00613-0 (2016).

16 Lasham, A. *et al.* A novel EGR-1 dependent mechanism for YB-1 modulation of paclitaxel response in a triple negative breast cancer cell line. *International journal of cancer* **139**, 1157-1170, doi:10.1002/ijc.30137 (2016).

17 Shajahan-Haq, A. N. *et al.* EGR1 regulates cellular metabolism and survival in endocrine resistant breast cancer. *Oncotarget* **8**, 96865-96884, doi:10.18632/oncotarget.18292 (2017).

18 Di Biase, S. *et al.* Fasting regulates EGR1 and protects from glucose- and dexamethasone-dependent sensitization to chemotherapy. *PLoS Biol* **15**, e2001951, doi:10.1371/journal.pbio.2001951 (2017).
19 Di Leva, G. *et al.* Estrogen mediated-activation of miR-191/425 cluster modulates tumorigenicity of breast cancer cells depending on estrogen receptor status. *PLoS Genet* **9**, e1003311, doi:10.1371/journal.pgen.1003311 (2013).
20 Hawley, S. A. *et al.* Phosphorylation by Akt within the ST loop of AMPK-alpha1 down-regulates its activation in tumour cells. *The Biochemical journal* **459**, 275-287, doi:10.1042/BJ20131344 (2014).
21 Ando, S., Barone, I., Giordano, C., Bonofiglio, D. & Catalano, S. The Multifaceted Mechanism of Leptin Signaling within Tumor Microenvironment in Driving Breast Cancer Growth and Progression. *Frontiers in oncology* **4**, 340, doi:10.3389/fonc.2014.00340 (2014).
22 Brandhorst, S. *et al.* A Periodic Diet that Mimics Fasting Promotes Multi-System Regeneration, Enhanced Cognitive Performance, and Healthspan. *Cell metabolism* **22**, 86-99, doi:10.1016/j.cmet.2015.05.012 (2015).
23 Wei, M. *et al.* Fasting-mimicking diet and markers/risk factors for aging, diabetes, cancer, and cardiovascular disease. *Sci Transl Med* **9**, doi:10.1126/scitranslmed.aai8700 (2017).
24 Arends, J. *et al.* ESPEN guidelines on nutrition in cancer patients. *Clin Nutr* **36**, 11-48, doi:10.1016/j.clnu.2016.07.015 (2017).
25 Arends, J. *et al.* ESPEN expert group recommendations for action against cancer-related malnutrition. *Clin Nutr* **36**, 1187-1196, doi:10.1016/j.clnu.2017.06.017 (2017).
26 Grundmann, O., Yoon, S. L. & Williams, J. J. The value of bioelectrical impedance analysis and phase angle in the evaluation of malnutrition and quality of life in cancer patients--a comprehensive review. *European journal of clinical nutrition* **69**, 1290-1297, doi:10.1038/ejcn.2015.126 (2015).
27 Turner, N. C. *et al.* Palbociclib in Hormone-Receptor-Positive Advanced Breast Cancer. *The New England journal of medicine* **373**, 209-219, doi:10.1056/NEJMoa1505270 (2015).
28 Creighton, C. J. *et al.* Insulin-like growth factor-I activates gene transcription programs strongly associated with poor breast cancer prognosis. *Journal of clinical oncology : official journal of the American Society of Clinical Oncology* **26**, 4078-4085, doi:10.1200/JCO.2007.13.4429 (2008).
29 Karey, K. P. & Sirbasku, D. A. Differential responsiveness of human breast cancer cell lines MCF-7 and T47D to growth factors and 17 beta-estradiol. *Cancer research* **48**, 4083-4092 (1988).
30 Baselga, J. *et al.* Everolimus in postmenopausal hormone-receptor-positive advanced breast cancer. *The New England journal of medicine* **366**, 520-529, doi:10.1056/NEJMoa1109653 (2012).
31 Andre, F. *et al.* Alpelisib for PIK3CA-Mutated, Hormone Receptor-Positive Advanced Breast Cancer. *The New England journal of medicine* **380**, 1929-1940, doi:10.1056/NEJMoa1813904 (2019).
32 Hu, R., Hilakivi-Clarke, L. & Clarke, R. Molecular mechanisms of tamoxifen-associated endometrial cancer (Review). *Oncology letters* **9**, 1495-1501, doi:10.3892/ol.2015.2962 (2015).
33 Ciribilli, Y. *et al.* The coordinated p53 and estrogen receptor cis-regulation at an FLT1 promoter SNP is specific to genotoxic stress and estrogenic compound. *PloS one* **5**, e10236, doi:10.1371/journal.pone.0010236 (2010).
34 Liu, C. Y. *et al.* Tamoxifen induces apoptosis through cancerous inhibitor of protein phosphatase 2A-dependent phospho-Akt inactivation in estrogen receptor-negative human breast cancer cells. *Breast cancer research : BCR* **16**, 431, doi:10.1186/s13058-014-0431-9 (2014).

35 Massarweh, S. *et al.* Tamoxifen resistance in breast tumors is driven by growth factor receptor signaling with repression of classic estrogen receptor genomic function. *Cancer research* **68**, 826-833, doi:10.1158/0008-5472.CAN-07-2707 (2008).
36 Mishra, A. K., Abrahamsson, A. & Dabrosin, C. Fulvestrant inhibits growth of triple negative breast cancer and synergizes with tamoxifen in ERalpha positive breast cancer by up-regulation of ERbeta. *Oncotarget* **7**, 56876-56888, doi:10.18632/oncotarget.10871 (2016).
37 Ikeda, H. *et al.* Combination treatment with fulvestrant and various cytotoxic agents (doxorubicin, paclitaxel, docetaxel, vinorelbine, and 5-fluorouracil) has a synergistic effect in estrogen receptor-positive breast cancer. *Cancer science* **102**, 2038-2042, doi:10.1111/j.1349-7006.2011.02050.x (2011).
38 Massarweh, S. *et al.* Mechanisms of tumor regression and resistance to estrogen deprivation and fulvestrant in a model of estrogen receptor-positive, HER-2/neu-positive breast cancer. *Cancer research* **66**, 8266-8273, doi:10.1158/0008-5472.CAN-05-4045 (2006).
39 Vijayaraghavan, S. *et al.* CDK4/6 and autophagy inhibitors synergistically induce senescence in Rb positive cytoplasmic cyclin E negative cancers. *Nature communications* **8**, 15916, doi:10.1038/ncomms15916 (2017).
40 Cook Sangar, M. L. *et al.* Inhibition of CDK4/6 by Palbociclib Significantly Extends Survival in Medulloblastoma Patient-Derived Xenograft Mouse Models. *Clinical cancer research : an official journal of the American Association for Cancer Research* **23**, 5802-5813, doi:10.1158/1078-0432.CCR-16-2943 (2017).
41 Michaloglou, C. *et al.* Combined Inhibition of mTOR and CDK4/6 Is Required for Optimal Blockade of E2F Function and Long-term Growth Inhibition in Estrogen Receptor-positive Breast Cancer. *Molecular cancer therapeutics* **17**, 908-920, doi:10.1158/1535-7163.MCT-17-0537 (2018).
42 Lee, C. *et al.* Reduced levels of IGF-I mediate differential protection of normal and cancer cells in response to fasting and improve chemotherapeutic index. *Cancer research* **70**, 1564-1572, doi:10.1158/0008-5472.CAN-09-3228 (2010).
43 Ahima, R. S. *et al.* Role of leptin in the neuroendocrine response to fasting. *Nature* **382**, 250-252, doi:10.1038/382250a0 (1996).
44 Di Biase, S. *et al.* Fasting-Mimicking Diet Reduces HO-1 to Promote T Cell-Mediated Tumor Cytotoxicity. *Cancer Cell* **30**, 136-146, doi:10.1016/j.ccell.2016.06.005 (2016).
45 Lee, C. *et al.* Fasting cycles retard growth of tumors and sensitize a range of cancer cell types to chemotherapy. *Sci Transl Med* **4**, 124ra127, doi:10.1126/scitranslmed.3003293 (2012).
46 Reidy, P. T. *et al.* Protein blend ingestion following resistance exercise promotes human muscle protein synthesis. *The Journal of nutrition* **143**, 410-416, doi:10.3945/jn.112.168021 (2013).
47 Rossi, F., Valdora, F., Barabino, E., Calabrese, M. & Tagliafico, A. S. Muscle mass estimation on breast magnetic resonance imaging in breast cancer patients: comparison between psoas muscle area on computer tomography and pectoralis muscle area on MRI. *European radiology* **29**, 494-500, doi:10.1007/s00330-018-5663-0 (2019).